IEEE Access
Multidisciplinary | Rapid Review | Open Access Journal

Received March 26, 2018, accepted April 29, 2018, date of publication May 3, 2018, date of current version June 5, 2018.

Digital Object Identifier 10.1109/ACCESS.2018.2832980

A Multicast Technique for Fixed and Mobile Optical Wireless Backhaul in 5G Networks

MICHAEL ATAKORA, (Member, IEEE), AND HARSHA CHENJI, (Member, IEEE)
School of Electrical Engineering and Computer Science, Ohio University, Athens, OH 45701, USA

Corresponding author: Harsha Chenji (chenji@ohio.edu)

This work was supported by the National Science Foundation under Grant CNS-1657279.

ABSTRACT The data demand for 5G networks is expected to be much higher than current throughput requirements. To meet this demand, a dense topology of interlinked small cells is needed. Laying new copper and fiber in such a dense network would be cost prohibitive. There is, therefore, an urgent need for high capacity wireless point-to-multipoint backhaul solutions. In this paper, we provide a compendium of solutions for ultrahigh data rate physical-layer broadcast and multicast using free space optics in 5G backhaul networks. We show that the problem of optimal multicast in mobile scenarios with highly directional optical links is a time-dependent prize collecting traveling salesman problem which is NP-hard. In formulating our problem, we develop a novel prize assignment strategy that guarantees the selection of mutually non-disjoint multicast sets. Due to the problem being NP-hard, we provide several potential heuristics for multicast in fixed and mobile scenarios, and present a comprehensive performance evaluation of the developed schemes.

INDEX TERMS Free space optics, multicast, 5G, backhaul, set cover, traveling salesman problem.

I. INTRODUCTION

The upcoming 3GPP 5G standard is designed to provide several gigabits per second throughput to users. The recent availability of several GHz of spectrum in the millimeter wave range is a key enabler of this throughput. 5G networks are envisioned to have a node density of about 50 BSs/km^2 [1]. This densification of cellular networks, combined with high throughput links, leads to interference. In order to manage interference and to ensure coverage in indoor and challenged environments, the concept of femto-, atto-, pico-cells and several other small cells have been proposed. However, these cells need to be interlinked - and the cost of laying new fiber or copper is extremely high. Therefore, there is an urgent immediate need for high capacity wireless backhaul solutions. These backhaul links cannot be fixed point-to-point wireless, but they need to support point-to-multipoint (using beam steering or other techniques) to accommodate Quality of Service and other constraints.

The 3GPP standards for LTE specify the Evolved Multimedia Broadcast and Multicast Service interface; it is anticipated that the corresponding demand in 5G will be much higher. Another interesting application of high data rate wireless point-to-multipoint communication is in datacenters where fiber is replaced by laser-based free space optical (FSO) links [2], [3]; data replication occurs in applications such as MapReduce and redundant storage. In mobile delay tolerant networks [4], replicating a packet to multiple nodes during a contact opportunity is very important.

While mmWave backhaul links have been investigated, we propose the use of FSO links for several reasons. First, compared to mmWave (tens of milliradians), the beamwidth is much smaller (μrad range) and therefore supports *higher densification*. Second, the entire optical spectrum is license free, with several THz of freely available spectrum. Third, inexpensive commercial off-the-shelf equipment can be used to establish multi-Gbps FSO links (e.g., Koruza [5]). This development is largely due to the availability of cheap fiber optic communication hardware - FSO links can be established by removing the optic fiber cable [6]. Fourth, laser communication has been demonstrated [7] at distances exceeding 100km, and at bit rates exceeding 80Gbps (though not simultaneously) in both static and mobile scenarios. In fact, the NASA LLCD project recently demonstrated an Earth-Moon optical link. These success stories continue to happen: Facebook very recently demonstrated an 80 Gbps, 13 km free space optical cross-link designed for use as backhaul in platforms such as OpenCellular.

Laser data rates are very high mainly because the beamwidth is very small [8]. Trying to reduce the link alignment time by widening the beam has the unwanted side effect of heavily reduced data rate. Thus there is a fundamental tradeoff between data rate and alignment delay. This problem is not very apparent in point-to-point links where the latter is incurred only once when the link is initially setup. Unfortunately this delay is incurred *multiple times* in backhaul networks where senders frequently talk to multiple receivers (e.g., during broadcast). In such networks it is essential to address this problem before trying to improve capacity by deploying highly directional links.

Motivated by the need for multimedia broadcast and multicast at ultra high data rates, we investigate the problem of physical layer multicasting (as opposed to multicast routing) in free space optical networks. We expand upon our previous work on FSO multicast in static scenarios [9] and emulated static conditions in mobile delay tolerant networks [4], [10]. While static multicast was shown to be NP-hard through reduction to Set Cover, we show that mobile multicast is an instance of the Time-Dependent Prize Collecting Traveling Salesman problem. The rest of this paper is organized as follows: we put our work in context with related efforts and present scenarios in which our developed solutions can be applied to in Section II. In Section III, we present a brief review of performing optimal multicast in static environments, whiles mobility is covered in Section IV. In Section V, drawing from our solutions for static and mobile scenarios, we compare solutions for both scenarios, and the effectiveness of using one solution for an environment it was not designed for. In the same section, we formulate heuristics meant to support mobile multicast. An evaluation of the various multicast schemes is presented in Section VI, after which we provide a conclusion.

II. APPLICABLE SCENARIOS & RELATED WORK

Multicasting in directional networks (whether RF, mmWave or optical) has been investigated in the state of art. In this section we first describe our application scenario (5G backhaul) through the use of expository examples, and summarize past and ongoing work. Static and mobile scenarios are differentiated and described in detail. Then, we provide a summary of related work across the spectrum, and show that our work is unique in several aspects. Contributions of this article are summarized, and is differentiated from our previous work [4], [9], [10].

A. APPLICABLE SCENARIOS

We now present some scenarios in which multicast can be used when nodes are either static or mobile.

1) STATIC MULTICAST

With the ever growing demand for data traffic, 5G and other next generation wireless systems, cannot completely rely on macro cells to support the increase in data capacity. A dense deployment of small cells having a range of at most a few hundred meters is widely recognized as the direction to proceed in addressing increasing data capacity demands [11]–[13]. A major challenge that has to be confronted with such a dense deployment of small cells is the provision of a backhaul network connecting these cells to the core network. Obviously, a wired backhaul would not only be expensive, but would also be unscalable [14]–[16]. There is therefore the need to make provision for a cost-effective and scalable backhaul network that does not use the already congested sub 3 GHz portion of the electromagnetic spectrum. In [15], [17], and [18], the use of millimeter-wave (mmWave) backhaul links in the unlicensed 60 GHz band and licensed 70 to 80 GHz band between macro and picocells and among picocells has been explored. With mmWave backhaul systems, data is aggregated from multiple users within the coverage area of a small cell's base station (S-BS) and routed via multiple high capacity mmWave backhaul links to the macrocell's base station (M-BS) which then forwards it to the core network. Point to multipoint backhaul networks [15], [17]–[20] allow for a low latency and cost effective 5G inter-BS reconfigurable wireless backhaul since any required link can be created on demand by virtue of either beam steering or beam switching as opposed to setting up $\mathcal{O}(n^2)$ dedicated links to connect n BSs. The use of hybrid RF/FSO as a backhaul solution for 5G wireless systems has been investigated [21]–[23]. Multicast can be leveraged in improving the latency and throughput of high capacity wireless optical backhaul networks for 5G communications and other next generation technologies.

2) MOBILE MULTICAST

In networks with highly directional transceivers, mobility introduces challenges with respect to maintaining links during a communications period. Pointing, acquisition, and tracking of the optical beam needs to be precise so as to preserve the link's existence. Facebook's plan to beam the Internet to rural and hard to reach areas using laser equipped solar powered drones [24]–[26] is a possible scenario whereby multicasting can improve throughputs. The basic concept of Facebook's proposed approach is presented in Figure 1. A network is formed between high altitude drones linked to a ground based Internet gateway via a ''mother'' drone. The drones relay Internet payload between themselves using high speed optical links and they serve their target communities with Internet via radio.

B. RELATED WORK

Over the last few years, many researchers have explored areas such as highly directional multicasting and wireless optical mobile ad-hoc networks. In this section, we present these related efforts and compare how they differ with the work presented in this paper.

The multicast problem in energy-aware and energy-limited RF networks is addressed in static scenarios using tree construction algorithms [27]–[31], [35]–[44]. These efforts do not tackle mobility. Optimal link layer multicasting

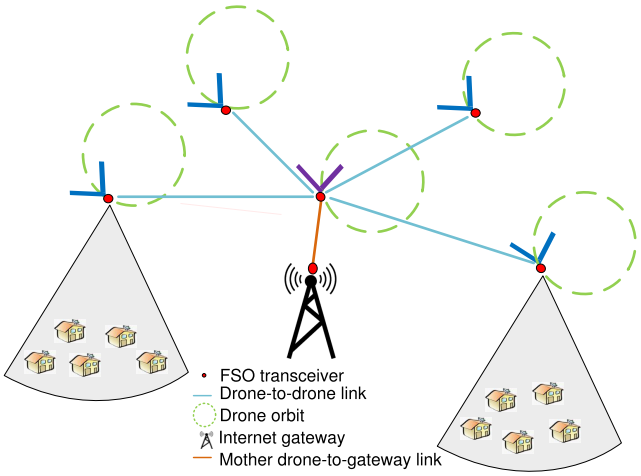

FIGURE 1. Possible application of mobile multicast: A high altitude platform for Internet access in rural communities.

in indoor static RF wireless networks using antennas with switched beamforming capabilities is achieved in [88] by manipulating the power across the composite beam's main lobes. For static mmWave wireless networks, [45] proposes an adjustable beamwidth mechanism which maximizes the data rate of receiving nodes. In the area of directional multicast in RF-based adhoc networks, the approach in [32]–[34] and [84], [85] use switchable antennas with fixed patterns in mobile and static environments respectively. The use of directional antenna systems in vehicular networks has been widely studied [70], [75], [82], [83]. Zhang *et al.* [75] study the multicast throughput capacity in directional RF antenna based vehicular ad hoc networks subject to delay constraints. Using a linear highway vehicular mobility model, a protocol for the dissemination of broadcast data from a static base station along the road to mobile vehicles is developed [82]. The protocol incorporates a mechanism to select relay vehicles in a manner that maximizes broadcast throughput.

In [54]–[63], the authors introduce and implement a FSO node design in which spherical surfaces are tessellated with several transceivers to attain near omnidirectional node coverage. They achieve this by means of an auto-alignment circuit that detects a loss of line of sight by electronically tracking optical beams. These efforts use LEDs which have divergence angles far greater than that of lasers used in our work. Using the tessellated transceiver design, [64], [65] design a distance vector routing protocol for hybrid RF/FSO based mobile adhoc networks. An evaluation of the impact of directional communications on ad hoc networks running dynamic source routing is presented [74].

The issue of link maintenance [46]–[53] in wireless optical mobile networks, although addressed, is limited to just a pair of nodes. In [51] and [52], inclinometer sensors and GPS are used to obtain a node's position for coarse alignment, whiles [46]–[50] uses an inband approach comprising of directional transceivers sending beacon signals to achieve the same objective. Reference [53] explores improving connectivity using adaptive divergence and transmit powers. With respect to RF, [70] explores using beam steerable directional antennas to improve link stability between mobile vehicles and a static base station.

The issue of medium access control (MAC) in RF-based directional wireless networks has been well investigated [73], [76]–[79], [87]. [73], [76] explores and addresses challenges in MAC protocol design stemming from interference due to the higher ranges of directional transmissions. Steenstrup [87] develop a TDMA-based MAC protocol that maximizes the number of concurrent sessions in the network. For the improvement of the lifetime of an ad hoc wireless network, coordination of transmissions is required. In [71], this is made possible using electronically steerable directional antennas to develop an energy-efficient routing and scheduling algorithm.

The authors of [66]–[69] develop algorithms for unicast networks with fragile optical links. The objective of such algorithms is the minimization of a transient information level metric defined to be a function of both the amount of information in the network and the projected physical distance to the destination, where constraints such as Quality of Service (QoS), varied network traffic, transmission and storage limits are incorporated into the algorithm. To meet QoS requirements such as latency and throughput, adaptive control of power and beamwidth is explored in [72] for topology control in hybrid RF/FSO mesh networks.

We draw from a number of concepts such as the ability to perform directional multicasting, usage of a single directional steerable transceiver, the adjustment of beamwidth and mobility in building our multicast algorithms in highly directional optical networks. In Table 1, we categorize related efforts using the concepts we build on in our work. We indicate which concepts or techniques were used (with a ✓). In Table 1, optical refers to the use of wireless optical transceivers such as LEDs and lasers, directional multicast refers to using multicasting in directional networks as opposed to performing omnidirectional broadcast, tracking refers to the ability for the transmitted beam to follow the trajectory of mobile nodes, steerable refers to using a single transceiver which can be guided to point in any direction, rather than a switchable antenna system whereby the direction in which the antenna system points to can be manipulated by changing which antenna is active. A single directional beam means that, there is only one active beam per transmitter whiles the adjustable beamwidth category refers to the ability to change the beamwidth of the transceiver on the fly.

Our main contributions in this paper is the development of a compendium of solutions for multicast over free space optical links in static and mobile scenarios. We expand upon our previous work on FSO multicast in static scenarios [9] and emulated static conditions in mobile delay tolerant networks [4], [10]. This effort is different from our work in [4], [9], and [10] mainly due to the consideration of mobility. In this paper (Section IV) we provide a generalized

TABLE 1. Summary of related research efforts.

Paper	Optical	Directional Multicast	Tracking	Steerable	Switchable	Single Active Directional Beam (Antenna Element)	Adjustable Beamwidth	Mobility
[27], [28], [29], [30], [31]		✓		✓			✓	
[32]		✓	✓		✓	✓		✓
[33], [34]		✓	✓		✓			✓
[35], [36], [37], [38], [39], [40], [41], [42], [43], [44]		✓		✓		✓	✓	
[45]		✓		✓			✓	
[46], [47], [48], [49], [50], [51], [52], [53]	✓		✓	✓		✓		✓
[54], [55], [56], [57], [58], [59], [60], [61], [62], [63], [64], [65]	✓		✓		✓			✓
[66], [67], [68], [69]	✓		✓	✓				✓
[70]			✓		✓			✓
[71]				✓		✓		
[72]	✓						✓	
[73]		✓		✓		✓		
[74], [75]		✓	✓	✓		✓		✓
[76]				✓		✓		
[77]					✓			
[78], [79]			✓		✓			✓
[80]				✓	✓	✓		
[81]			✓	✓	✓	✓		✓
[82], [83]		✓				✓		✓
[84], [85]		✓			✓			
[86]		✓			✓	✓		
[87]		✓	✓					✓
[88]		✓		✓	✓		✓	
Our work	✓	✓	✓	✓		✓	✓	✓

solution for achieving optimal multicast in *mobile* networks via a translation of the problem to the Time-Dependent Prize Collecting Salesman Problem.

III. OPTIMAL MULTICAST: THE STATIC SCENARIO

In this section we review our static multicast algorithms from [9], [10]. We provide a background into the FSO PHY, describe concepts such as broadcast and multiple unicast which ultimately lead us to formulating the static FSO multicast problem. We then provide an exact solution and a faster but approximate greedy heuristic.

A. PRELIMINARIES

The beam generated at the FSO source either diverges due to physical imperfections in the source, or can be made to diverge using a lens; this angle of divergence is defined as the *beam divergence angle* θ (Figure 2a). Given L as the Euclidean distance between the sender and receiver, the effective data rate R_b at a divergence angle of θ is expressed [89] as

$$R_b(\theta) = \frac{P_r}{hfN_b} = \frac{P_t D^2 L_{tp} L_{rp} \eta_t \eta_r 10^{\frac{-\alpha L}{10^4}}}{hfN_b \theta^2 L^2} \quad (1)$$

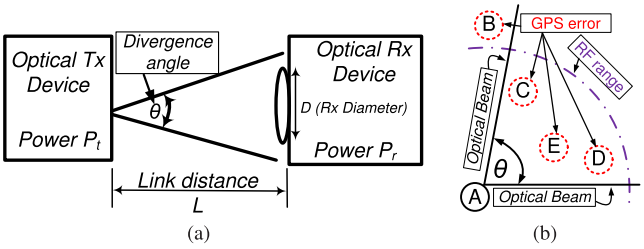

FIGURE 2. (a) Illustrating various FSO link parameters for a point-to-point link: P_t, P_r, L, θ and D. (b) A RF+FSO network where A talks with C, D & E with a FSO beam divergence of θ. A is unaware of B since it is outside of A's RF radio range. (a) FSO Link. (b) RF+FSO Net.

where P_t is the transmitted power, D is the receiver diameter, L_{tp} and L_{rp} are the pointing losses resulting from imperfect alignment of the transmitter and receiver respectively, η_t and η_r are the transmitter and receiver optical efficiencies respectively, α is the atmospheric attenuation factor, f is the frequency of the light source, h is Planck's constant and N_b is the detector sensitivity. The RF+FSO system model is shown in Figure 2b. The nodes ("A,B,C,D,E" in Figure 2b) are equipped with an omnidirectional RF radio as well as a directional FSO radio. Nodes broadcast their position over RF.

We account for possible positioning errors (dotted line around nodes in Figure 2b), since GPS systems currently have a 3m position accuracy g 95% of the time. Therefore, nodes have to set θ such that the receiver is within the FSO footprint. Nodes outside the RF range (''B'' in Figure 2b) are not considered as neighbors since their location cannot be obtained.

B. SYSTEM MODEL: BROADCAST VS. MULTIPLE UNICAST

The fundamental building blocks to formulating the static multicast problem are the concepts of broadcast and multiple unicast which are based on the ability to manipulate beam divergence and steer the laser transmitter. With broadcast (Figure 3a) the transmitter's θ is manipulated so that all receivers are within its footprint. In the case of multiple unicast (Figure 3b), data is sent to each receiver one at a time with non-zero alignment delay d_{al} accounted for. We define d_{al} as the time it takes a node to perfectly reorient it's laser transmitter in the direction of another node. We use our understanding of broadcast and multiple unicast to obtain all possible multicast combinations. We define a universe $\mathcal{U}$ of nodes that are to receive broadcast data. A *set* S_i is a group of nodes in the network whereby exactly one transmission is required to multicast to each of it's elements. It is noted that the union of all sets S_i should be equal to $\mathcal{U}$. A hybrid combination of sets is presented in Figure 3c whereby the first multicast transmission is a broadcast to B & C with the second transmission being a unicast to D.

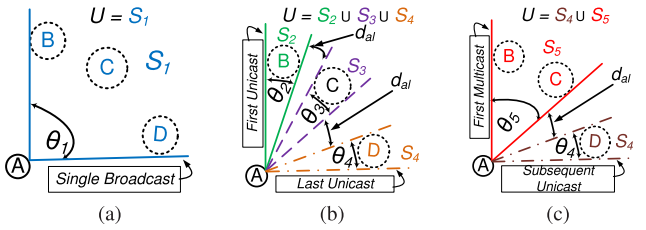

FIGURE 3. Illustrating several set combinations in FSO multicast (a) a broadcast set with a FSO beam divergence angle of θ_1 (b) multiple (three) unicasts with divergence angles of θ_2, θ_3 and θ_4 (c) a hybrid of broadcast and unicast sets. The union of all sets in a diagram is always equal to the universe of nodes. (a) A set with all receivers (B, C and D). (b) A possible combination of sets. (c) Another combination of subsets.

The minimum number of multicast sets K can be derived by sorting receivers in order of decreasing azimuth ϕ from the origin (where node A is located) and observing that, whiles following a clockwise trajectory, if ϕ_i for node i is less than ϕ_j for node j, and greater than ϕ_k for node k, and if $j, k \in S_x$, then node $i \in S_x$. Using this structure to enumerate all possible sets for a given $\mathcal{U}$ from Figure 3, we see that there is exactly 1 set of size 3 (S_1), exactly 3 sets of size 1 (S_2, S_3, S_4), and exactly 3 sets of size 2 (S_5, $S_6 = \{C, D\}$ and $S_7 = \{D, B\}$, S_6 & S_7 are not shown in Figure 3).Therefore generally, to broadcast to N nodes, there are exactly N sets of size 1 through to size $N-1$, and exactly 1 set of size N, for a total of $K = N^2 - N + 1$. The constructed sets lead us to the static FSO multicast problem (S-FSOMP).

C. STATIC MULTICAST PROBLEM FORMULATION

The static FSO multicast problem can be stated as follows: given a universe $\mathcal{U} = \{n_1, n_2, \ldots, n_N\}$ of N nodes, a collection $\mathcal{S} = \{S_1, S_2, \ldots, S_K\}$ of $K = N^2 - N + 1$ sets can be constructed. The cost of broadcasting data to a set S_i is the data delivery delay d_i which depends on R_b for that set, which in turn depends on the required θ. The objective is to find $\mathcal{S}' \in \mathcal{S}$ with minimum total delay such that all N nodes are covered. The delivery delay d_i for a set S_i is computed using the size of the broadcast data P, the minimum divergence angle θ_i required for all member nodes to be in the transmitter's footprint, and alignment delay d_{al}. Using Equation 1, d_i is calculated as

$$d_i = \max_j \left\{ \frac{P}{R_b(\theta_i)} + d_{al} \right\} \text{ where } 1 \leq j \leq |S_i| \tag{2}$$

where $R_b(\theta_i)$ is calculated for each node $j \in S_i$ using different values of distance L_j. We formulate the optimal FSO multicast problem as a 0/1 integer problem. Each set S_i is assigned a binary decision variable: x_i is 1 if $S_i \in \mathcal{S}'$, and 0 otherwise. The problem can now be formulated as follows.

Problem 1: The Static FSO Multicast Problem

$$\textit{minimize} \sum_{i=1}^{K} x_i d_i \tag{3}$$

$$\textit{subject to} \bigcup S_j = \mathcal{U} \quad \forall \quad S_j \in \mathcal{S}'$$

$$\textit{where } S_i \in \mathcal{S}' \textit{ if } x_i = 1 \tag{4}$$

In the objective (Equation 3), the delay d_i per set is the cost (Equation 2) of sending data to all nodes in that set. Equation 4 stipulates that each node has to be in at least one set. Taking into account the structure of constructed multicast sets, we see that that optimal solution to S-FSOMP consists of mutually disjoint sets (see Theorem 1).

D. THE EXACT STATIC MULTICAST SOLUTION (S-SC)

We translate the Static FSO Multicast Problem (S-FSOMP) into a Minimum Weighted Set Cover (MWSC) problem. Formally, the MWSC problem is as follows. Given a universe $\mathcal{U}$ of N elements, and a collection $\mathcal{S} = \{S_1, S_2, \ldots, S_K\}$ of sets whose elements are in $\mathcal{U}$, where each set S_i is assigned a weight w_i, the objective is to find a subset $\mathcal{S}'$ of $\mathcal{S}$ with minimum total weight such that each element in $\mathcal{U}$ exists in at least one set in $\mathcal{S}'$ (i.e., all elements are ''covered''). We can easily see that S-FSOMP is equivalent to the MWSC problem.

Theorem 1: The exact minimum weighted set cover (MWSC) solution to S-FSOMP guarantees the selection of mutually disjoint multicast sets.

Proof: Suppose for the sake of contradiction that there exists a sequence of multicast transmissions $\mathcal{D} = \{D_1, D_2, \ldots, D_K\}$ with optimal total cost $C(\mathcal{D})$ which contains a pair of mutually non-disjoint sets (D_1, D_2). We let θ_{D_1}, $C(D_1)$ and θ_{D_2}, $C(D_2)$ represent the divergence angle and cost associated with sending data to sets D_1 and D_2 respectively. In addition, we let $D_{12} = D_1 \cap D_2$, and form two new sets F_1 and F_2 s.t. $F_1 = D_1 - D_{12}$ and $F_2 = D_2$. F_1

and F_2 have θ_{F_1}, $C(F_1)$ and θ_{F_2}, $C(F_2)$ as divergence angle and cost respectively. A new sequence of disjoint multicast transmissions $\mathcal{F} = \{F_1, F_2, \ldots, F_K\}$ is created from $\mathcal{D}$ s.t. $F_i = D_i$ when $i \geq 3$. With the structure of multicast sets obtained via the azimuthal ordering of receivers, we see that $\theta_{F_1} < \theta_{D_1}$. Since $C(S_i) \propto \theta_{S_i}^2$, $C(F_1) < C(D_1)$, hence $C(\mathcal{F}) < C(\mathcal{D})$. Since there is a sequence of disjoint multicast sets $\mathcal{F}$ whose total cost is guaranteed to be smaller than $\mathcal{D}$, we establish the contradiction that $\mathcal{D}$ represents an optimal solution. □

E. THE APPROXIMATE STATIC MULTICAST SOLUTION

The approximate solution S-AP to the static free space optical multicast problem is based on the standard $O(\log N)$ set cover approximation algorithm in [90].We present the solution in (Algorithm 1).

Algorithm 1 The Approximate Set Cover Algorithm (S-AP)

Input: A universe $\mathcal{S} = \{S_1, S_2, \ldots, S_K\}$ of $K = N^2 - N + 1$ sets
Output: A subcollection of sets $\mathcal{S}'$ that covers the universe of $\mathcal{U} = \{n_1, n_2, \ldots, n_N\}$ of N nodes

1 $\mathcal{S}' \leftarrow \emptyset$
2 $\mathcal{U}' \leftarrow \emptyset$
3 **for** $S_j \in \mathcal{S}$ *s.t.* $j \leftarrow 1$ ***to*** K **do**
4 compute d_j using Equation 2
5 $j^* = \min_j \frac{d_j}{|S_j|}$
6 $\mathcal{S}' \leftarrow S_{j^*}$
7 $\mathcal{U}' \leftarrow S_{j^*}$
8 **while** $\mathcal{U}' \neq \mathcal{U}$ **do**
9 **for** $S_j \notin \mathcal{S}'$ **do**
10 $\frac{d_j}{|S_j|} \leftarrow \frac{d_j}{|S_j - \mathcal{U}'|}$
11 $j^* = \min_j \frac{d_j}{|S_j|}$
12 $\mathcal{S}' \leftarrow \mathcal{S}' \bigcup S_{j^*}$
13 $\mathcal{U}' \leftarrow \mathcal{U}' \bigcup S_{j^*}$

S-AP takes as input the collection of all K sets. The set cover is initially empty as seen in lines 1, and 2. In line 4, the cost effectiveness $\frac{d_j}{|S_j|}$ of selecting a set S_j into the cover is initialized. S-AP works by greedily picking the most cost-effective set (smallest cost per uncovered set elements) in each iteration till all nodes are covered. In lines 6, 7, the most cost effective set is chosen into the cover. Whiles all nodes are not covered (lines 8 - 13), the cost effectiveness of a set is updated to reflect the cost associated with currently uncovered nodes (line 10). The most cost effective set is then placed in the cover. This process continues until all nodes are covered. This algorithm has a time complexity of $O(N^2)$ if linear search is used to obtain the most cost effective set relative to covering previously uncovered nodes.

Theorem 2: The approximate minimum weighted set cover (S-AP) solution to S-FSOMP guarantees the selection of mutually disjoint multicast sets.

Proof: Suppose for the sake of contradiction that Algorithm 1 selects a pair of mutually non-disjoint sets (S_1, S_2) from the collection $\mathcal{S}$ of K multicast sets. We let θ_{S_1}, $C(S_1)$ and θ_{S_2}, $C(S_2)$ represent the divergence angle and cost associated with sending data to sets S_1 and S_2 respectively. We further assume that Algorithm 1 picks S_1 first. In other words, S_1 is the most cost effective set in lines 4 - 7. For the sake of simplicity, we assume that S_2 is picked immediately after S_1. In addition, we let $S_{12} = S_1 \cap S_2$, and form a new set F_1 s.t. $F_1 = S_2 - S_{12}$ with θ_{F_1}, $C(F_1)$ as divergence angle and cost (Equation 2) respectively. With the structure of multicast sets obtained via the azimuthal ordering of receivers, we note that $F_1 \in \mathcal{S}$. With S_2 containing at least all nodes in F_1, we observe that $\theta_{S_2} > \theta_{F_1}$ which translates to $C(F_1) < C(S_2)$. In addition to this, it is clear that after S_1 is picked, $|S_2 - S_1| = |F_1 - S_1|$. Therefore S_2 cannot be picked in the next iteration since $\frac{C(S_2)}{|S_2 - S_1|} > \frac{C(F_1)}{|F_1 - S_1|}$. This process can be repeated for any pair of selected sets. We have thereby established via contradiction that Algorithm 1 always yields mutually disjoint sets. □

Algorithm 2 Greedy Local Optimum Heuristic (S-HEU)

Input: Location (x_i, y_i) for nodes n_1 **to** n_N, P, d_{al}
Output: Sets containing nodes in multicast group

1 **for** $i \leftarrow 1$ ***to*** N **do**
2 $\phi_i \leftarrow tan(\frac{y_i - y_0}{x_i - x_0})$
3 Sort nodes in clockwise order of ϕ_i to obtain $n_{1'}$ **to** $n_{N'}$
4 $j \leftarrow 1$
5 $S_j \leftarrow n_{1'}$
6 **for** $i \leftarrow 1'$ ***to*** $N' - 1$ **do**
7 **if** $d_{i',i'+1} < d_{i'} + d_{i'+1} + d_{al}$ **then**
8 $S_j \leftarrow S_j \bigcup n_{i'+1}$
9 **else**
10 $j \leftarrow j+1$
11 $S_j \leftarrow n_{i'+1}$

Due to the computational complexity associated with the integer program formulation of the problem and the $O(N^2)$ S-AP(Algorithm 1), these solutions might not be ideal for highly dense mobile networks where the network topology changes frequently. We therefore provide a greedy heuristic (Algorithm 2). The heuristic builds sets by greedily comparing the cost of broadcasting to that of multiple unicast to a pair of adjacent nodes. The delay $d_{i',i'+1}$ associated with broadcasting to a pair of adjacent nodes $n_{i'}$ and $n_{i'+1}$ is defined as the weight d (Equation 2) of a set $S = \{n_{i'}, n_{i'+1}\}$. Similarly, the delay $d_{i'}$ associated with unicasting to a node $n_{i'}$ is defined as $P/R_b(\theta_{i'})$. In lines 1 to 3, the sender sorts the receivers in clockwise order of azimuth ϕ_i from the origin (sender's location). A set is then created and the first

node in the array of sorted nodes is placed in it (lines 4,5). In lines 6 to 11, the algorithm compares the delay associated with broadcasting to a pair of adjacent nodes to that of multiple unicast. Nodes are placed in sets depending on which scheme is cheaper (lines 8-11).

IV. OPTIMAL MULTICAST: THE MOBILE SCENARIO

In Section III, we considered only instances where nodes where static and it was assumed that the sender of the multicast data was known, with all receivers pointing in the direction of the sender. Mobility introduces complexity into the design of multicast algorithms for mobile networks, hitherto not associated with multicast in static environments. With mobility, the cost associated with sending data to nodes in a set is a function of time. This is because R_b is no longer constant, but depends on time varying θ, $\theta(t)$ and time varying transmitter to receiver distances $L(t)$. In addition to identifying the sets to use for multicast, the order of consecutive transmissions also has an effect on the optimality of the multicast solution. The FSO Multicast Problem with Mobility (M-FSOMP) can be stated as follows: given a universe $\mathcal{N} = \{n_1, n_2, \ldots, n_N\}$ of N nodes, a collection $\mathcal{S} = \{S_1, S_2, \ldots, S_K\}$ of $K = N^2 - N + 1$ sets can be constructed. The cost of broadcasting data to a set S_i is the data delivery delay d_i which depends on a time varying R_b for that set, which in turn depends on the required $\theta(t)$. The objective is to find an ordered sequence of disjoint transmissions $\mathcal{S}' \in \mathcal{S}$ with minimum total delay such that all N nodes receive broadcast data.

A. THE TIME-DEPENDENT PRIZE COLLECTING TRAVELING SALESMAN PROBLEM (TDPCTSP)

We show that an instance of M-FSOMP can be translated into a Prize Collecting Traveling Salesman Problem (PCTSP) [91]–[93] with time-dependent edge weights. The time-dependence of edge weights gives rise to the Time-Dependent Prize Collecting Traveling Salesman Problem (TDPCTSP). Formally TDPCTSP is stated as follows. Given a list of cities, a prize w_l at city l to be collected if visited, a penalty h_l if city l is not visited, and a time-dependent cost $c_{uv}(t)$ between cities u and v, the objective is to find a tour of a subset of these cities such that the total cost and penalty is minimized, subject to the collection of a certain prize w_T.

In constructing the TDPCTSP instance, we create $K + 1$ ''virtual'' nodes. The first virtual node v_0 is the origin of the cycle (i.e. the sender of broadcast data in M-FSOMP). Each of the remaining K virtual nodes correspond to a unique multicast set in $\mathcal{S}$. In other words, we represent sets as virtual nodes in the TDPCTSP instance. The universe of virtual nodes $\mathcal{V} = \{v_0, v_1, v_2, \ldots, v_K\}$ excluding the origin v_0 maps directly to the collection of multicast sets $\mathcal{S} = \{S_1, S_2, \ldots, S_K\}$ (i.e. v_1 corresponds to S_1, v_2 corresponds to S_2, …, v_K corresponds to S_K). In broadcast networks, data replication to the same node, apart from scenarios whereby a packet does not reach its next hop needs to avoided since it represents a wastage of network resources. With this in mind, the optimal solution to the M-FSOMP has to consist of mutually disjoint multicast sets. To ensure that all receiving nodes get broadcast data exactly once during a session, the trick in the TDPCTSP instance is to develop a prize assignment strategy that guarantees that all valid tours have the same unique total prize, whiles invalid tours have a prize not equal to the prize of any valid tour.

Definition 1: A valid tour $\mathcal{T}$ is a cycle of $\mathcal{V}' \in \mathcal{V}$ visited virtual nodes with respect to the sending node X s.t., $\bigcup S_j = \mathcal{N} \quad \forall \quad v_j \in \mathcal{V}'$ and $S_i \bigcap S_j = \emptyset \quad \forall \quad v_i, v_j \in \mathcal{V}'$ where $i \neq j$.

Definition 2: An invalid tour is a cycle of $\mathcal{V}' \in \mathcal{V}$ visited virtual nodes with respect to the sending node X s.t., $\bigcup S_j \neq \mathcal{N} \quad \forall \quad v_j \in \mathcal{V}'$ or $S_i \bigcap S_j \neq \emptyset \quad \forall \quad v_i, v_j \in \mathcal{V}'$ where $i \neq j$.

In the next subsection we present a prize assignment strategy that guarantees that the solution to the TDPCTSP is a valid tour.

B. TDPCTSP PRIZE ASSIGNMENT STRATEGY

In this subsection, we present a way to assign prizes to virtual nodes that guarantees the selection of a valid tour as the solution to the TDPCTSP instance. Fist and foremost, we form a basis set $\mathcal{R}$ of virtual nodes from $\mathcal{V}$. $v_j \in \mathcal{R}$ if and only if $|S_j| = 1 \forall \quad v_j \in \mathcal{V}$ and $j \geq 1$. It is clearly seen that $|\mathcal{R}| = N$. We assign to each $R_l \in \mathcal{R}$ a basis prize $b_l = \log p_l$ where p_l is a prime number unique to R_l. We define the prize w_j for virtual node v_j as follows

$$w_j = \begin{cases} 0 & \text{if} j = 0 \\ \sum_{l:R_l \in \mathcal{S}_j} b_l & \text{if} j \geq 1 \end{cases} \tag{5}$$

The total prize of a valid tour w_T is therefore

$$w_T = \sum_{l:R_l \in \mathcal{R}} b_l \tag{6}$$

Theorem 3: The prize assignment $w_j = \sum_{l:R_l \in \mathcal{S}_j} b_l$ guarantees that the TDPCTSP instance selects mutually disjoint multicast sets.

Proof: Suppose the prizes of virtual nodes in the TDPCTSP instance are assigned using Equation 5, we will show that Equation 5 guarantees the selection of mutually disjoint multicast sets in the TDPCTSP solution. In doing this, first and foremost, we prove that all valid tours yield a total prize of w_T. In addition to this, we also prove that no invalid tour can have a total prize of w_T.

The intuition behind our proof lies in the Fundamental Theorem of Arithmetic [94], which states that every positive integer can be uniquely represented as the product of prime numbers. From the definition of valid tours in Definition 1, we observe that a valid tour only contains exactly N receivers each present in exactly 1 multicast set. Since each receiver appears exactly once in a valid tour, each receiver is clearly in $\mathcal{R}$. With each $R_l \in \mathcal{R}$ uniquely assigned a basis prize $b_l = \log p_l$ where p_l is a unique prime number, the total prize of the

basis w_b is $w_b = \log \prod_{l:R_l \in \mathcal{R}} p_l$. The term $\prod_{l:R_l \in \mathcal{R}} p_l \in \mathbb{Z}_{>1}$, hence, as a consequence of the Fundamental Theorem of Arithmetic, it is uniquely prime factorable. It is easy to see that the logarithm of all factors of $\prod_{l:R_l \in \mathcal{R}} p_l$ yields the basis prizes b_l. The total prize of the basis w_b, $w_b = \sum_{l:R_l \in \mathcal{R}} b_l = w_T$ where w_T is the total prize for a valid tour in Equation 6. We have shown that a valid tour always yields a total prize of w_T, hence the first part of the proof is complete.

The second part of the proof pertains to invalid tours. We provide a proof by way of contradiction. We suppose that there is an invalid tour with total prize w_T. As seen from the first part of the proof, by assigning logarithms of primes to basis virtual nodes and using the Fundamental Theorem of Arithmetics, a total prize of w_T is attainable if and only if there are exactly N unique receivers each present in exactly 1 multicast set. Clearly, this is a contradiction since invalid tours either have at least a pair of mutually non exclusive sets or do not contain N distinct receivers.

We have shown that the prize assignment $w_j = \sum_{l:R_l \in \mathcal{S}_j} b_l$ preserves the selection of mutually disjoint multicast sets in the TDPCTSP instance. The proof is complete. □

C. TIME-DEPENDENT COST FUNCTION

In this subsection we develop a time-dependent cost function for the assignment of edge weights. This is necessary because with mobility, the cost of sending data to a multicast set is not constant over time, but depends on the positions of nodes in the set relative to the sender during the transmission period. To account for the fluctuations in instantaneous data rate, we use the average data rate $\overline{R_b(t)}$ over a transmission period to estimate the per set data delivery delay. $R_b(t)$ for node j in set S_i is expressed as

$$R_b(t) = \frac{M 10^{\frac{-\alpha L_j(t)}{10^4}}}{\theta_{S_i}(t)^2 L_j(t)^2} \tag{7}$$

where $M = \frac{P_t D^2 L_{tp} L_{rp} \eta_t \eta_r}{hf N_b}$, $\theta_{S_i}(t)$ is the time-varying divergence angle for set S_i, and $L_j(t)$ is the time-varying distance from the receiving node j to the sender X.

In Figures 4a to 4c, we illustrate effect of mobility on time-dependent edge weights. We consider a static transmitter and a mobile receiver moving at a speed of 2 m/s away from the transmitter and initially located 20 m from it (as is the case in Figure 4a). For the sake of analysis we use $P_t = 60$ mW, $g = 8$ m, $N_b = 6$ photons/bit. As the receiver gets farther away from the transmitter, θ per the set containing the single receiver decreases (Figure 4b). This is because the farther a node moves from the transmitter, the smaller the θ required to meet g becomes (see Subsection III-A). We also observe from Figure 4b that $\frac{\Delta\theta_{rA}}{\Delta t_{rA}} > \frac{\Delta\theta_{rB}}{\Delta t_{rB}}$ where rA and rB represent regions A and B respectively. In region A, $\frac{\Delta\theta_{rA}}{\Delta t_{rA}} \gg \frac{\Delta\theta_{rB}}{\Delta t_{rB}}$ than that of region B, so θ has a greater influence on $R_b(t)$ compared to the TX-RX distance L_j. However in region B, $\frac{\Delta\theta_{rB}}{\Delta t_{rB}}$ is very small, hence, $R_b(t)$ depends largely on L_j. This explains the trend in Figure 4c.

$\overline{R_b(t)}$ over a transmission period is

$$\overline{R_b(t)} = \frac{1}{t_f - t_s} \int_{t_s}^{t_f} R_b(t)\, dt \tag{8}$$

with t_s and t_f such that

$$P = \int_{t_s}^{t_f} R_b(t)\, dt \tag{9}$$

P is the data sent per transmission period. The average cost $\overline{d_i}$ per set S_i is

$$d_i = \max_j \left\{ \frac{P}{\overline{R_b}} + d_{al} \right\} \text{ where } 1 \le j \le |S_i| \tag{10}$$

where $\overline{R_b}$ is calculated for each node $j \in S_i$ using different values of distance L_j and d_{al} is the alignment delay.

We use the previously developed set weights (Equations 7 - 10) to come up with an edge weight assignment scheme for the TDPCTSP instance. We formulate our problem on a complete directed graph $\mathcal{G} = (\mathcal{V}, \mathcal{E})$ where virtual nodes $u \in \mathcal{V}$ and edges $(u, v) \in \mathcal{E}$. In performing the translation from M-FSOMP to TDPCTSP, to make the notation easy to follow, we let S_u correspond to virtual node u. The time-dependent edge weight $c_{uv}(t)$ for a pair of virtual nodes $u, v \in \mathcal{V}$ is the cost of sending data to virtual node v (set S_v) immediately after sending data to virtual node u (set S_u). $c_{uv}(t)$ is expressed as

$$c_{uv}(t) = \begin{cases} \max\limits_j \left\{ \frac{P}{\overline{R_b}} + d_{al} \right\} & \text{where } 1 \le j \le |S_v| \\ \infty, & S_u \bigcap S_v \neq \emptyset \\ 0, & \text{if } v = X \end{cases} \tag{11}$$

The data arrival time at virtual node v in the TDPCTSP instance (i.e. the time S_v in M-FSOMP receives data) is $t_v = t_u + c_{uv}$, where t_u is the time data arrived at the previous node in the salesman's path (i.e. the time the preceding set S_u in M-FSOMP receives data). Note that at the origin X, $t_u = 0$.

D. A M-FSOMP TO TDPCTSP EXAMPLE

In this subsection, we present a translation of a M-FSOMP scenario into an instance of TDPCTSP. Suppose node X intends to send data to nodes A and B as shown in Figure 5a, the objective is to find the sequence of multicast transmissions with minimum total data delivery delay. We assume that nodes X, A and B are mobile. In the M-FSOMP instance, the universe of receiving nodes is $\mathcal{N} = \{A, B\}$. With $N = |\mathcal{N}| = 2$, we then form $K = 3$ sets. The collection of sets $\mathcal{S} = \{\{A\}, \{B\}, \{A, B\}\}$. Each set is then associated with a virtual node. The universe of virtual nodes $\mathcal{V} = \{X, A, B, AB\}$. The basis for virtual nodes $\mathcal{R}$ is then $\mathcal{R} = \{A, B\}$. We assign prizes to each member of $\mathcal{R}$ as described in Subsection IV-B. Virtual nodes A, B and AB are assigned prizes of $\log 2$, $\log 3$ and $\log 6$ respectively. The prize of a valid tour w_T, which is the sum of the prizes assigned to elements (i.e A and B) in the basis. In this example, $w_T = \log 2 + \log 3 = \log 6$. A complete directed graph $\mathcal{G} = (\mathcal{V}, \mathcal{E})$ is then formed with $\mathcal{V} = \{X, A, B, AB\}$, and edge weights assigned using the cost

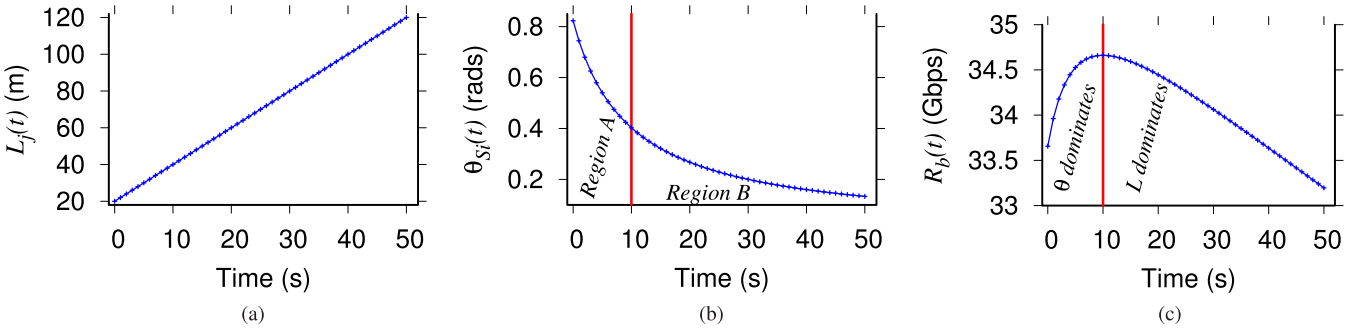

FIGURE 4. Illustrating the effect of node mobility on cost. (a) Time-dependent distance between a mobile receiver and a static transmitter, (b) Effect of mobility on divergence angle $\theta_{S_j}(t)$, (c) Effect of mobility on instantaneous data rate $R_b(t)$.

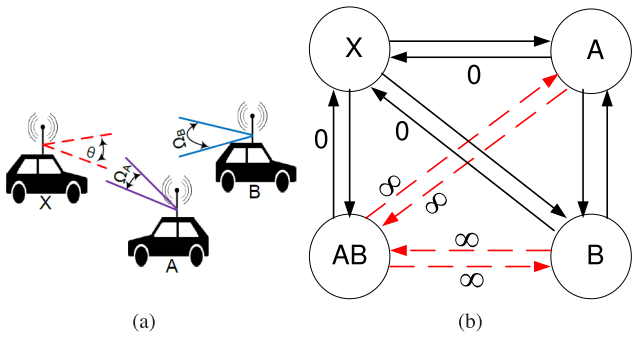

FIGURE 5. Conversion from M-FSOMP to TDPCTSP. (a) An instance of M-FSOMP whereby node X intends to send data to nodes A and B with field of views of Ω_A, Ω_B respectively, (b) An instance of the TDPCTSP with the objective of finding the shortest tour with respect to X to a subset of virtual nodes subject to prize constraints.

function in Equation 11. As an example, all edges terminating on X are assigned a 0 weight whiles edges connecting mutually non disjoint virtual nodes (sets) are assigned a weight of ∞ (Figure 5b). The edge weight for a pair of mutually disjoint sets is time dependent.

E. M-FSOMP 0/1 INTEGER LINEAR PROGRAM FORMULATION

We now formulate the M-FSOMP as a 0/1 Integer Linear Program(ILP). The formulation is based on the PCTSP 0/1 ILP and the TDTSP 0/1 ILP presented in [91]–[93], [95], and [96] respectively. The problem can now be formulated as follows.

Problem 2: The FSO Multicast Problem with Mobility

$$\begin{aligned} &minimize\ z^* s_w + c^{z^*}_{u^* v^*} \\ &\quad with\ z^* = \max_{z \in \mathcal{Z}} |\quad x^z_{uv} = 1 \\ &\quad and\ u^* = u, v^* = v \quad at \quad x^{z^*}_{uv} = 1 \qquad (12) \\ &subjectto \sum_{v \in \mathcal{V} \setminus \{u\}} \sum_{z \in \mathcal{Z}} x^z_{uv} - y_u = 0 \quad \forall \quad u \in \mathcal{V} \qquad (13) \\ &\quad \sum_{u \in \mathcal{V} \setminus \{v\}} \sum_{z \in \mathcal{Z}} x^z_{uv} - y_v = 0 \quad \forall \quad v \in \mathcal{V} \qquad (14) \\ &\quad \sum_{(u,v) \in \mathcal{E}} x^z_{uv} \le 1 \quad \forall \quad z \in \mathcal{Z} \qquad (15) \end{aligned}$$

$$w_T - \epsilon \le \sum_{u \in \mathcal{V}} w_u y_u \le w_T + \epsilon \qquad (16)$$

$$\left(\sum_{(u,v) \in \mathcal{E}} x^{z_b}_{uv} \sum_{(u,v) \in \mathcal{E}} x^{z_a}_{uv} \right)$$

$$\left((z_b - z_a)\, s_w - d_{al} - \sum_{(u,v) \in \mathcal{E}} c^{z_a}_{uv} x^{z_a}_{uv} \right) \ge 0$$

$$\forall \quad z_a, z_b \in \mathcal{Z} \quad s.t. \quad z_b > z_a \qquad (17)$$

$$where\ y_u \in \{0, 1\};\ x^z_{uv} \in \{0, 1\};$$

$$u, v \in \mathcal{V};\ (u, v) \in \mathcal{E};\ z \in \mathcal{Z} \qquad (18)$$

In the objective (Equation 12), the time-dependent weight c^z_{uv} of edge (u, v) is obtained using a discretized version of Equation 11. c^z_{uv} is the average cost on edge (u, v) when data is sent at any time within slot z to multicast set (virtual node) v, immediately after a transmission to set u. To derive c^z_{uv}, it is necessary to obtain an upper bound t_{up} on the total time required to multicast data to all receivers. Since the total multicast cost for the optimum sequence of transmissions is upper bounded by the cost of any valid sequence of transmissions, t_{up} is basically the cost of a valid sequence (e.g. a sequence of unicast sets or a single broadcast set). With t_u for the first transmission t_{u1} in the sequence known (i.e. 0 s), $Z = |\mathcal{Z}|$ non-overlapping time slots each of width s_w are created from the t_{u1} to t_{up} interval with each time slot $z \in \mathcal{Z}$.

x^z_{uv} is 1 if edge (u, v) in time slot z is selected to be in the optimum tour and 0 if otherwise. y_u is 1 if virtual node u is selected to be in the optimum tour and 0 if otherwise. Since the prize collecting constraint (Equation 16) guarantees that all receivers in the M-FSOMP get the broadcast data, the penalty h_l incurred if virtual node l is not visited is set to 0. The constraints in Equation 13- 14 guarantee that any virtual node in the optimum tour has exactly one incoming and one outgoing edge. Constraint Equation 15 ensures that at most one edge is chosen per time slot. In other words, at most one transmission to a multicast set can begin in each time slot.The prize collecting constraint is given in Equation 16. Taking into account that w_T might be irrational because it is the sum of logarithms, we subject the total prize collected to a lower and upper bound of w_T.

In Equation 17, we introduce the alignment constraints. For a pair of slots z_a and z_b such that slot z_a precedes z_b, we formulate constraints that ensure that the commencement of a transmission in a selected slot only occurs at least d_{al} seconds after the end of the preceding transmission. We observe that since $z_b > z_a$, there are $\frac{Z(Z-1)}{2}$ such constraints with each having $\mathcal{O}(|\mathcal{V}|^2|)$ terms.

V. COMPARISON BETWEEN S-FSOMP AND M-FSOMP

We present a comparison between the solutions developed to address multicast in static and mobile scenarios. Using the same procedure in Subsection IV-A, it is easy to see that S-FSOMP can be translated into an instance of PCTSP. We briefly present an alternative to the MWSC formulation of S-FSOMP.

Problem 3: S-FSOMP as a PCTSP

$$minimize \left(\sum_{u\in\mathcal{V}} \sum_{v\in\mathcal{V}\setminus\{u\}} (c_{uv}+d_{al})x_{uv} + \sum_{u\in\mathcal{V}} h_u(1-y_u) \right) - d_{al} \tag{19}$$

$$subjectto \sum_{v\in\mathcal{V}\setminus\{u\}} x_{uv} - y_u = 0 \quad \forall \quad u \in \mathcal{V} \tag{20}$$

$$\sum_{u\in\mathcal{V}\setminus\{v\}} x_{uv} - y_v = 0 \quad \forall \quad v \in \mathcal{V} \tag{21}$$

$$w_0 - \epsilon \leq \sum_{u\in\mathcal{V}} w_u y_u \leq w_0 + \epsilon \tag{22}$$

$$where\ y_u \in \{0,1\}; x_{uv} \in \{0,1\}$$
$$u, v \in \mathcal{V}; (u,v) \in \mathcal{E} \tag{23}$$

The symbols, constraints, and variables are identical to those in Problem 2, with the only difference being the exclusion of time-dependent variables and constraints. Note that in the objective(Equation 19) of S-FSOMP, the alignment delay d_{al} is factored into the cost of a multicast set. Bearing in mind that a sequence of Q consecutive multicast transmissions incurs Q-1 aligment delays, we subtract one d_{al} in the objective. S-FSOMP in Problem 3 contains $\mathcal{O}(|\mathcal{V}|^2)$ variables and $\mathcal{O}(|\mathcal{V}|)$ constraints whiles the equivalent formulation in Problem 1 uses $\mathcal{O}(|\mathcal{V}|^2)$ variables and $\mathcal{O}(N)$ constraints. With the TDPCTSP formulation of M-FSOMP, the total number of variables involved is $\mathcal{O}(|\mathcal{V}|^2|\mathcal{Z}|)$, with $\mathcal{O}(Z^2)$ constraints assuming $|\mathcal{Z}| \gg |\mathcal{V}|$. Clearly, TDPCTSP can be used to solve S-FSOMP, however due to its larger number of variables and constraints, it is more computationally complex to solve relative to using either the MWSC or PCTSP formulations in static scenarios. Due to the M-FSOMP being NP-hard, in the next few subsections, we provide heuristics to solve the mobile multicast problem based on two main approaches: a mobile time dependent greedy heuristic, and mobile heuristics based on static approaches.

A. MOBILE TIME-DEPENDENT GREEDY HEURISTIC

The time-dependent greedy heuristic (M-TDH, Algorithm 3) described in this subsection is fundamentally similar to Algorithm 2 for the static case, with the main difference being the incorporation of time-dependent set weights. Algorithm 3 takes as input the universe of K sets and yields an ordered subcollection of sets $\mathcal{S}''$. In lines 1 to 2, the prize associated with each set(virtual node) is computed. The total prize of covering each node is computed in lines 3 to 4. A running total prize w_R, and the current cover are initialized in lines 5 to 7. At the initial start time for a session, the time dependent weights for each set is computed (lines 8 to 9). The most cost effective set is chosen and placed in the cover, the finish time t_f of the first transmission is initialized, and the running total prize updated (lines 10 to 14). In lines 15 to 23, whiles the total prize has not been met, the cost effectiveness of each set is updated and the most effective set placed in the cover. This process repeats itself till the total prize is met. Note that, similar to Theorem 2, this algorithm yields mutually disjoint sets.

Algorithm 3 Time-Dependent Greedy Heuristic (M-TDH)

Input: A universe $\mathcal{S} = \{S_1, S_2, \ldots, S_K\}$ of $K = N^2 - N + 1$ sets
Output: An ordered subcollection of sets $\mathcal{S}''$ that covers the universe of $\mathcal{U} = \{n_1, n_2, \ldots, n_N\}$ of N nodes

1 **for** $S_j \in \mathcal{S}$ *s.t.* $j \leftarrow 1$ ***to*** K **do**
2 compute w_j using Equation 5
3 **for** $n_x \in \mathcal{U}$ *s.t.* $x \leftarrow 1$ ***to*** N **do**
4 compute w_T using Equation 6
5 $w_R \leftarrow 0$
6 $\mathcal{S}'' \leftarrow \emptyset$
7 $\mathcal{U}'' \leftarrow \emptyset$
8 At initial start time $t_s zt_0$, **for** $S_j \in \mathcal{S}'$ *s.t.* $j \leftarrow 1$ ***to*** K **do**
9 compute d_j using Equation 10
10 $j^* = \min_j \frac{d_j}{|S_j|}$
11 $\mathcal{S}'' \leftarrow S_{j^*}$
12 $\mathcal{U}'' \leftarrow S_{j^*}$
13 $t_f \leftarrow t_s + d_{j^*}$
14 $w_R \leftarrow w_{j^*}$
15 **while** $w_R \neq w_T$ **do**
16 **for** $S_j \in \mathcal{S}$ **do**
17 update d_j at $t_s = t_f$ using Equation 10
18 $\frac{d_j}{|S_j|} \leftarrow \frac{d_j}{|S_j - \mathcal{U}''|}$
19 $j^* = \min_j \frac{d_j}{|S_j|}$
20 $\mathcal{S}'' \leftarrow \mathcal{S}'' \bigcup S_{j^*}$
21 $\mathcal{U}'' \leftarrow \mathcal{U}'' \bigcup S_{j^*}$
22 $t_f \leftarrow t_s + d_{j^*}$
23 $w_R \leftarrow w_R + w_{j^*}$

B. MOBILE HEURISTICS BASED ON STATIC APPROACHES

In our previous works [4], [9], [10], we introduced static multiple unicast (S-MU), the static optimal set cover solution (S-SC), the static local optimum heuristic (S-HEU),

and the standard approximation algorithm to the set cover solution (S-AP) to optimize multicast in static and emulated static conditions in mobile networks. In this subsection, we describe a greedy approach to mobile multicast using solutions obtained from static schemes. As established in Theorem 1, Theorem 2, by the definition of multiple unicast (Subsection III-B) and the operation of the heuristic(Subsection 2), S-SC, S-AP, S-MU and S-HEU all yield mutually disjoint multicast sets. The algorithm (Algorithm 4) takes as input the sets computed by the static schemes and yields an ordered collection of these sets. In lines 3 to 7, the most cost effective set at the start of the multicast session is chosen and placed into the new cover. The time the transmission to this set is complete is computed in line 8. In lines 9 to 16, the cost effectiveness of each set is updated and the most cost effective (least cost per uncovered elements) chosen. Note that the input sets to the algorithm are mutually disjoint. This process of iterative picking sets continues till a complete ordered collection of sets is obtained.

Algorithm 4 Mobile Multicast Based on Static Set Selection

Input: A subcollection of sets $\mathcal{S}'$ based on the output of either S-MU, S-SC, S-HEU, S-AP

Output: An ordered subcollection of sets $\mathcal{S}''$

1 $\mathcal{S}' \leftarrow \emptyset$
2 $\mathcal{U}' \leftarrow \emptyset$
3 At initial start time $t_s = t_0$, **for** $S_j \in \mathcal{S}'$ *s.t.* $j \leftarrow 1$ ***to*** $|\mathcal{S}'|$ **do**
4 compute d_j using Equation 10
5 $j^* = \min_j \frac{d_j}{|S_j|}$
6 $\mathcal{S}'' \leftarrow S'_{j^*}$
7 $\mathcal{U}'' \leftarrow S'_{j^*}$
8 $t_f \leftarrow t_s + d_{j^*}$
9 **while** $\mathcal{S}''$ - $\mathcal{S}' \neq \mathcal{S}'$ - $\mathcal{S}''$ **do**
10 **for** $S_j \in \mathcal{S}'$ **do**
11 update d_j at $t_s = t_f$ using Equation 10
12 $\frac{d_j}{|S_j|} \leftarrow \frac{d_j}{|S_j - \mathcal{U}'|}$
13 $j^* = \min_j \frac{d_j}{|S_j|}$
14 $\mathcal{S}'' \leftarrow \mathcal{S}'' \bigcup S_{j^*}$
15 $\mathcal{U}'' \leftarrow \mathcal{U}'' \bigcup S_{j^*}$
16 $t_f \leftarrow t_s + d_{j^*}$

VI. PERFORMANCE EVALUATION

In this section, we analyze results for various mobile multicast schemes: multiple unicast (S-MU) which greedily performs N unicasts, our proposed time-dependent heuristic (Algorithm 3) and the optimal set cover solution with greedy modifications (S-SC, III-D and Algorithm 4). We do not present results for S-AP and S-HEU since they were very identical to S-SC. The reason being that S-SC, S-AP and S-HEU are all inherently based on static set selections and as such yield similar results when applied to a mobile scenario. For a performance comparison of S-SC, S-AP and S-HEU in static and emulated mobile networks, we refer the interested reader to our previous work in [10].

A. SIMULATION SETUP

For the evaluation of the various multicast schemes, we simulate an optical 5G backhaul network whereby a static node (e.g. a 5G macro-cell base station on the roof top of a building) sends data to mobile nodes (e.g mobile 5G micro-cell base stations on trains). The mobile nodes randomly choose a destination, and move linearly towards it as illustrated in Figure 7. Mobile nodes move with speeds of 0 - 4 m/s. A single message (several GBs) was created at the static node and relayed to all mobile receivers. The mobile receivers were simulated to move away from the static node. Each receiving node is between 100 m and 200m from the sender at the commencement of the multicast session. We use a default of 10 mobile receiving base stations which translates to a base station density of node density of about 250 BSs/km^2. Our simulation environment was a Java based simulator which we built. In our work, we address issues that might arise when nodes enter or exit the network during an ongoing data transmission session to recipients. Assuming a new node comes into the network in the middle of a session, transmissions are not made to that new node. The new node becomes part of a new session when the current session is complete. In the case of a node leaving the network during a session, if that node has not yet received multicast data, the transmitter aborts data transfer to the node that has left.

We evaluate the performance of the solutions for this scenario using total delay and throughput as metrics. Each data point is the result of an average of 100 random runs. The parameters we use for the analysis are data size P, alignment delay d_{al}, receiver sensitivity N_b, localization error g,

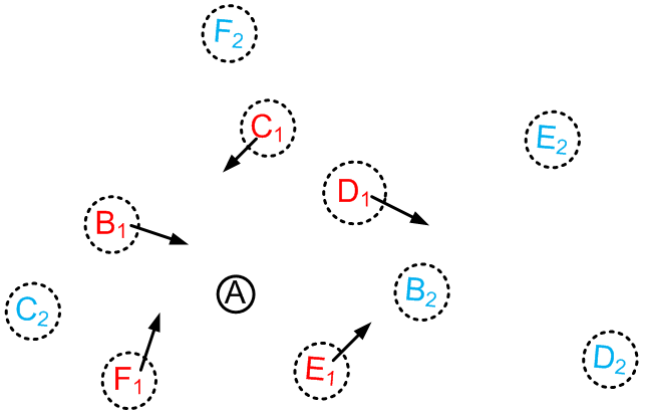

FIGURE 7. The mobility model used in the simulations. A static 5G macro-cell BS mounted on a roof top (node A) sends data to multiple 5G micro-cell BSs on trains (Nodes B to F). Nodes B to F at time t_1 choose random destinations where they move towards and arrive at time t_2 (denoted by locations $B_2 \ldots F_2$).

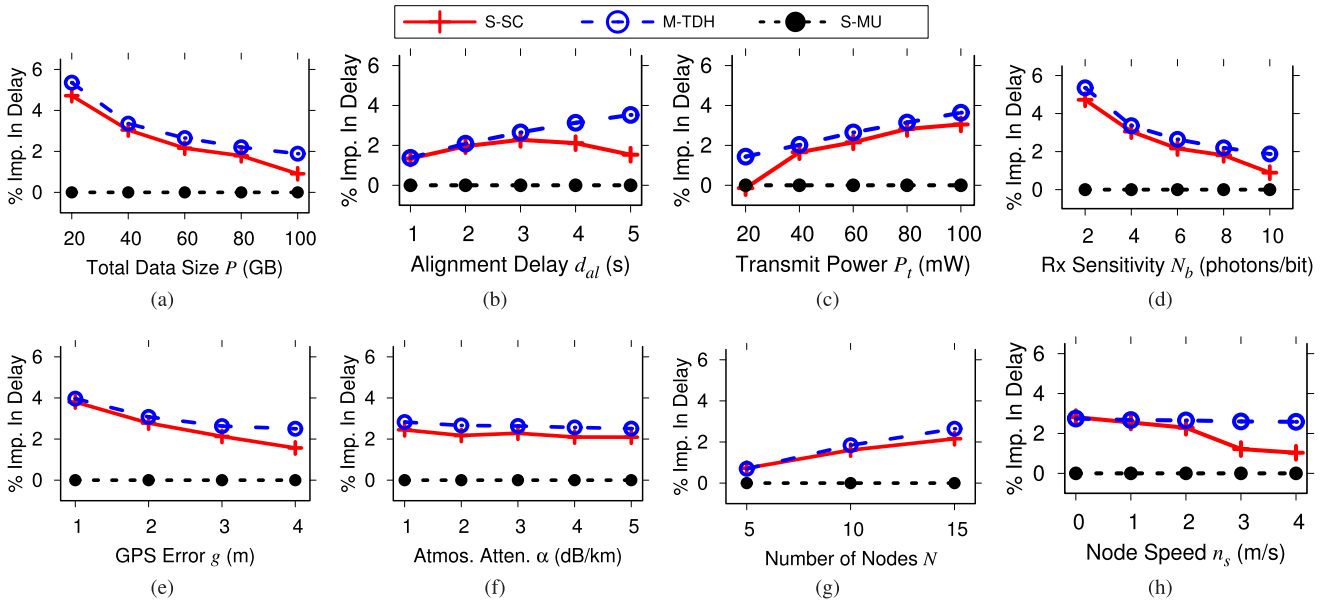

FIGURE 6. Percentage improvement in delay w.r.t. S-MU for different multicast approaches versus various network parameters. (a) Effect of P on delay for P = 20-100 GB, (b) Effect of d_{al} on delay for $d_{al} = 1 - 5$ s, (c) Effect of P_t on delay for P_t = 20-100 mW, (d) Effect of N_b on delay for N_b = 2-10 photons/bit, (e) Effect of g on delay for g = 1-4 m, (f) Effect of α on delay for α = 1-5 dB/km, (g) Effect of N on delay for N = 5-15, (h) Effect of n_s on delay for n_s = 0-4 m/s.

FSO transmit power P_t, number of mobile nodes N, atmospheric attenuation α, and node speed v_s. The default values (and ranges) used are: $P = 60$ GB (20-100 GB), $d_{al} = 3$ s (1-5 s), $N_b = 6$ photons/bit (2-10 photons/bit), $g = 3$ m (1-4m), $P_t = 60$ mW (20-100 mW), $N = 15$ (5-15), $v_s = 2$ m/s (0-4 m/s), $\alpha = 3$ dB/km (1-5 dB/km). In addition, we used a wavelength of 1550 nm, and a receiver diameter $D = 12$ mm.

B. DELAY AND AVERAGE THROUGHPUT

The delay metric quantifies the time required to relay data from the static node to all mobile receivers. We present delay results (Figures 6a to 6h) as percentage improvements over the S-MU baseline. We define average throughput to be aggregate throughput (total data transferred/total time taken) divided by the number of nodes. The effect of various parameters on average throughput is shown in Figure 8 again using percentage improvements over the S-MU baseline.

In addition to these figures, we make available in Table 2 raw data of the actual S-MU delay results which were used in the creation of Figures 6a to 6h. That being said, results in this section would be interpreted by jointly considering Figures 6a to 8h and Table 2.

Before we explain the results in detail, we first would like to provide an intuition as to why the performance improvements are generally less than 6%. With 15 nodes, a GPS accuracy g of 3m, and with each receiver at least 100 m from the sender at the start of the multicast session, the minimum divergence angle θ per node is about 0.06 rad. Since the transmitter is steerable, it has a 2π transmission footprint. Assuming that nodes are evenly distributed within this footprint, the angular azimuthal spatial separation between an ordered (anti)clockwise pair of receivers $|\phi_{i+1} - \phi_i|$ is approximately 0.42 rad. With $|\phi_{i+1} - \phi_i| \gg \theta$, and given the fact that $R_b \propto \theta^{-2}$,it is easy to see why algorithms would generally tend to yield multiple unicast set selections. In other words, node density plays a critical role in when receivers are grouped into sets.

TABLE 2. S-MU delay and throughput data used to compute the percentage improvements for the other schemes in Figures 6a to 8h.

P for Figures 6a and 8a

Metric	20 GB	40 GB	60 GB	80 GB	100 GB
Delay (s)	53.48	64.21	75.28	86.51	97.95
TPut (Gbps)	2.99	4.98	6.38	7.40	8.17

d_{aL} for Figures 6b and 8b

Metric	1 s	2 s	3 s	4 s	5 s
Delay (s)	46.67	60.96	75.28	89.60	103.92
TPut (Gbps)	10.29	7.87	6.38	5.36	4.62

P_t for Figures 6c and 8c

Metric	20 mW	40 mW	60 mW	80 mW	100 mW
Delay (s)	145.91	92.27	75.28	66.97	62.06
TPut (Gbps)	3.29	5.20	6.38	7.17	7.73

N_b for Figures 6d and 8d

Metric	2 ph/bit	4 ph/bit	6 ph/bit	8 ph/bit	10 ph/bit
Delay (s)	53.42	64.20	75.28	86.54	97.98
TPut (Gbps)	8.98	7.48	6.38	5.55	4.90

g for Figures 6e and 8e

Metric	1 s	2 s	3 s	4 s
Delay (s)	46.50	57.05	75.28	101.87
TPut (Gbps)	10.32	8.41	6.38	4.71

α for Figures 6f and 8f

Metric	1 dB/km	2 dB/km	3 dB/km	4 dB/km	5 dB/km
Delay (s)	72.14	73.60	75.28	77.09	79.07
TPut (Gbps)	6.65	6.52	6.38	6.27	6.07

N for Figures 6g and 8g

Metric	5	10	15
Delay (s)	22.76	48.84	75.28
TPut (Gbps)	21.09	9.83	6.38

v_S for Figures 6h and 8h

Metric	0 m/s	1 m/s	2 m/s	3 m/s	4 m/s
Delay (s)	73.92	74.51	75.28	76.17	77.09
TPut (Gbps)	6.49	6.44	6.38	6.30	6.23

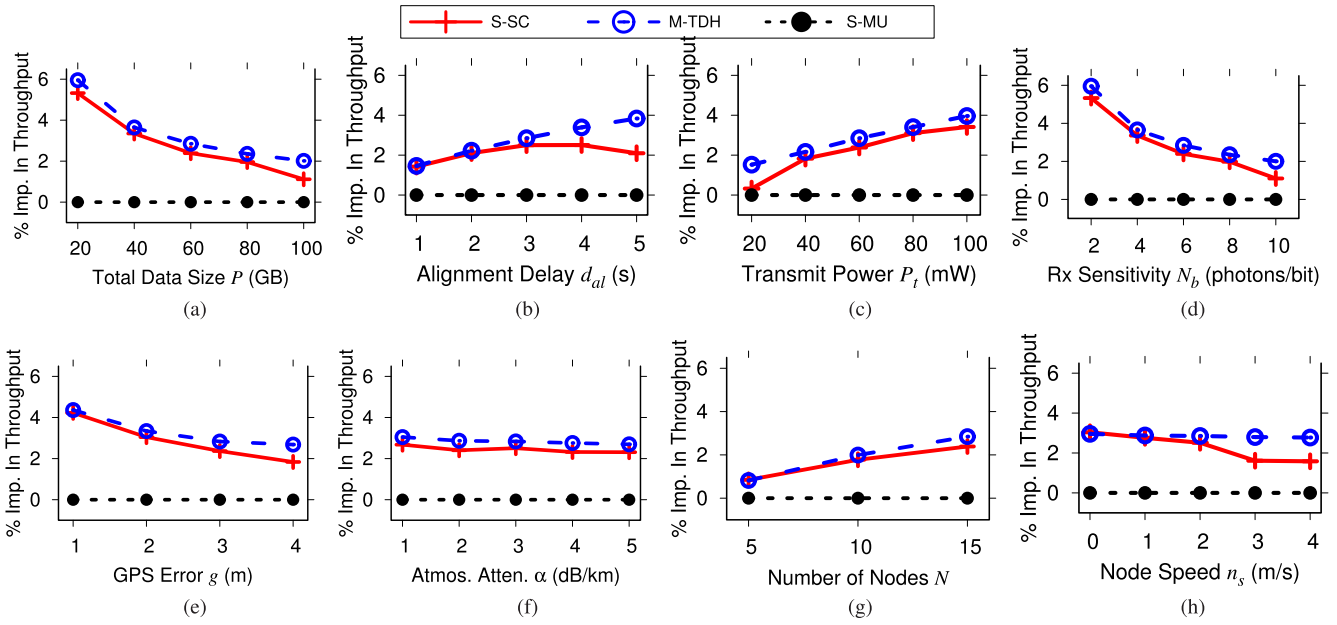

FIGURE 8. Percentage improvement in throughput w.r.t. S-MU for different multicast approaches versus various network parameters. (a) Effect of P on throughput for P = 20-100 GB, (b) Effect of d_{al} on throughput for d_{al} = 1-5 s, (c) Effect of P_t on throughput for P_t = 20-100 mW, (d) Effect of N_b on throughput for N_b = 2-10 photons/bit, (e) Effect of g on throughput for g = 1-4 m, (f) Effect of α on throughput for α = 1-5 dB/km, (g) Effect of N on throughput for N = 5-15, (h) Effect of n_s on throughput for n_s = 0-4 m/s.

In all our delay and throughput results, both M-TDH and S-SC perform better than S-MU. M-TDH has the best improvements in delay and throughput primarily because it is an inherently mobile multicast scheme. S-SC and S-MU on the other hand are schemes designed for static scenarios, but enhanced through a greedy ordering of selected sets to suit mobile scenarios. In Figures 6a and 8a, as data size P increases, delay increases and throughput decreases across all schemes. This is because the bigger the P, the longer the per set data transmission delay. This directly translates into a longer total delay (smaller throughput) per multicast session. We also observe that there is a decline in percentage improvements in delay and throughput as P grows larger. When P is small, $\frac{P}{R_b} \ll d_{al}$ for sets S_i with $|S_i| > 1$ and a dense intra angular separation of nodes. These sets tend to be chosen in the cover. For such sets, $|S_i| > 1$, hence there are fewer realignments relative to S-MU which suffers from $N-1$ realignments. This explains why performance improvements are higher at lower data sizes. At larger data sizes, $\frac{P}{R_b}$ and d_{al} are of similar orders of magnitude, resulting in a selection of mostly unicast sets.

The effect of alignment delay d_{al} on delay and throughput are evaluated in Figures 6b and 8b respectively. As expected, for the three schemes, an increase in d_{al} leads to a rise in total delay and a decline in throughput. This is due to the fact that the greater d_{al}, the longer it takes the last bit to reach the farthest recipient in the last set in the ordered collection of transmissions. As was the case in the relationship between data size P and the evaluated metrics, for large values of d_{al}, $\frac{P}{R_b} \ll d_{al}$, and sets with multiple constituent nodes are typically chosen. When d_{al} is large, $\frac{P}{R_b}$ and d_{al} are comparable, with unicasting being the likeliest outcome in such scenarios. M-TDH has the best improvement in delay and throughput because it factors in time-dependent set costs when greedily picking up sets to construct the cover.

A characterization of the impact transmit power P_t has on delay and throughput is presented in Figures 6c and 8c. There is a decrease in total delay (increase in throughput) for S-MU, S-SC and M-TDH as P_t increases. This is fairly intuitive since the per set transmission delay reduces with increasing P_t. The trend in Figures 6c and 8c can be explained by observing that sets which have sizes greater than 1 and have a dense spatial topology of nodes within it have the tendency to be selected as P_t grows. A reduction on the number of realignments over S-MU accounts for the rise in the improvements in delay and throughput of M-TDH and S-SC. With respect to transmit power, receiver sensitivity N_b has a reverse effect on delay and throughput. This is because, they are both scalars in Equation 1, and affect R_b in inverse ways. The reasons behind the trends in Figures 6c and 8c can be extended to support the trends in Figures 6d, and 8d.

We accounted for potential localization errors via the GPS accuracy parameter g. When g is known, the minimum divergence angle per set θ can be set in such a manner that the boundaries of the transmitted FSO beam are tangential to the circumference of the localization error region around nodes at the extreme edges of the set. Clearly for all schemes, an increase in g yields to a surge in delay and a reduction in throughput. The reason for this is, as g increases θ for all sets increases, leading to a reduction in R_b and an increase

in delay per set. Subsequently, the aggregate delay increases. M-TDH has a better improvement in delay and throughput over S-SC, with both schemes offering superior performance relative to S-MU in Figures 6e and 8e.

In discussing the effect of atmospheric attenuation α on delay and throughput, we consider the relationship between α and R_b in Equation 1. R_b depends on α exponentially. The 1-5 dB/km attenuation factors are typical to clear sky. α in that range does not significantly affect R_b. This explains the slight improvements in delay and throughput as seen in Figures 6f and 8f.

A network with a large number of receivers, incurs a larger total delay than a smaller one. In the case of S-MU, the reason is quite obvious, more sets (realignments) are required to reach all receivers. In the case of schemes in which the set size is not limited to a single node, generally as N increases, either the number of sets, the divergence angle per set, or both increase. This leads to a growth in delay and a fall in throughput. In relation to Figures 6g and 8g, an increase in N means greater node density. Greater node density further implies a larger pool of sets to pick the collection of consecutive transmissions from. As N grows, there is the tendency to select non unicast sets. This explains why at $N = 5$, there is just an approximately 0.8% improvement in delay and throughput for M-TDH as compared to a 2.8% improvement when $N = 15$.

In discussing the effect of node speed v_s on delay and throughput, we would leverage on concepts from Subsection IV-C. Using the results from Table 2, there is a slight increase in delay (decrease in throughput) as v_s increases from 0 to 4 m/s. Figure 4 shows a dependence of $R_b(t)$ for node j in set S_i on both the set's divergence $\theta_{S_i}(t)$ and its distance $L_j(t)$ from the sender. The closer a node is to the transmitter, the larger the θ_{S_i} and smaller the L_j is. Nodes farther away have a smaller θ_{S_i} but a larger L_j. With these dynamics, determining which of the two parameters has a larger influence on $R_b(t)$ can sometimes be intricate since $R_b(t)$ depends inversely with the square of both terms (see Equation 7).

VII. CONCLUSION

In this paper, we presented a compendium of multicast techniques which can be used for fixed and mobile optical wireless backhaul in 5G network. We showed that the optimal multicast problem can be translated time-dependent prize collecting traveling salesman problem. In formulating the optimal multicast problem with mobility, we developed a prize assignment strategy and proved that such a strategy guaranteed the selection of a valid tour of mutually non-disjoint multicast sets. With the problem known to be NP-hard, we provided and evaluated several potential heuristics for multicast in mobile scenarios.

ACKNOWLEDGMENT

Earlier version of this article appeared at Globecom 2016 and IWCMC 2017.

REFERENCES

[1] X. Ge, S. Tu, G. Mao, and C. X. Wang, "5g ultra-dense cellular networks," *IEEE Trans. Wireless Commun.*, vol. 23, no. 1, pp. 72–79, Feb. 2016.

[2] N. Hamedazimi *et al.*, "FireFly: A reconfigurable wireless data center fabric using free-space optics," in *Proc. ACM Conf. SIGCOMM*, 2014, pp. 319–330. [Online]. Available: http://doi.acm.org/10.1145/2619239.2626328

[3] J. Bao, D. Dong, B. Zhao, Z. Luo, C. Wu, and Z. Gong, "FlyCast: Free-Space optics accelerating multicast communications in physical layer," in *Proc. ACM Conf. Special Interest Group Data Commun. (SIGCOMM)*, 2015, pp. 97–98. [Online]. Available: http://doi.acm.org/10.1145/2785956.2790002

[4] M. Atakora and H. Chenji, "Overcoming alignment delay in RF+FSO networks," in *Proc. IEEE IWCMC Wireless Opt. Netw. Symp. (IWCMC WON Syposium)*, Valencia, Spain, Jun. 2017, pp. 628–633.

[5] *Koruza*. Accessed: Jan. 20, 2018. [Online]. Available: http://koruza.net/

[6] H. A. Willebrand and B. S. Ghuman, "Fiber optics without fiber," *IEEE Spectr.*, vol. 38, no. 8, pp. 40–45, Aug. 2001.

[7] D. W. Young, H. H. Hurt, J. E. Sluz, and J. C. Juarez, "Development and demonstration of laser communications systems," *John Hopkins APL Tech. Dig.*, vol. 33, no. 2, pp. 122–138, Sep. 2015.

[8] A. K. Majumdar, *Advanced Free Space Optics* (Springer Series in Optical Sciences), vol. 186. New York, NY, USA: Springer, 2015. [Online]. Available: http://link.springer.com/10.1007/978-1-4939-0918-6

[9] M. Atakora and H. Chenji, "Optimal multicasting in hybrid RF/FSO DTNs," in *Proc. IEEE Global Commun. Conf., Opt. Netw. Syst. (GLOBECOM ONS)*, Washington, DC, USA, Dec. 2016, pp. 1–6.

[10] M. Atakora and H. Chenji, "Multicast techniques for hybrid RF/FSO DTNs," *J. Opt. Commun. Netw.*, vol. 9, no. 11, pp. 1051–1061, Nov. 2017.

[11] "Small cells whats the big idea?" Small Cell Forum Ltd, London, U.K., Tech. Rep., Feb. 2012.

[12] "Enabling hyper-dense small cell deployments with UltraSON," Qualcomm Technol. Inc., San Diego, CA, USA, Tech. Rep., Feb. 2014.

[13] N. Bhushan *et al.*, "Network densification: The dominant theme for wireless evolution into 5G," *IEEE Commun. Mag.*, vol. 52, no. 2, pp. 82–89, Feb. 2014.

[14] S. Chia, M. Gasparroni, and P. Brick, "The next challenge for cellular networks: Backhaul," *IEEE Microw. Mag.*, vol. 10, no. 5, pp. 54–66, Aug. 2009.

[15] S. Hur, T. Kim, D. J. Love, J. V. Krogmeier, T. A. Thomas, and A. Ghosh, "Millimeter wave beamforming for wireless backhaul and access in small cell networks," *IEEE Trans. Commun.*, vol. 61, no. 10, pp. 4391–4403, Oct. 2013.

[16] Z. Zhang, X. Wang, K. Long, A. V. Vasilakos, and L. Hanzo, "Large-scale MIMO-based wireless backhaul in 5G networks," *IEEE Wireless Commun.*, vol. 22, no. 5, pp. 58–66, Oct. 2015.

[17] C. Dehos, J. L. González, A. De Domenico, D. Kténas, and L. Dussopt, "Millimeter-wave access and backhauling: The solution to the exponential data traffic increase in 5G mobile communications systems?" *IEEE Commun. Mag.*, vol. 52, no. 9, pp. 88–95, Sep. 2014.

[18] X. Ge, H. Cheng, M. Guizani, and T. Han, "5G wireless backhaul networks: Challenges and research advances," *IEEE Netw.*, vol. 28, no. 6, pp. 6–11, Nov. 2014.

[19] R. Taori and A. Sridharan, "Point-to-multipoint in-band mmwave backhaul for 5G networks," *IEEE Commun. Mag.*, vol. 53, no. 1, pp. 195–201, Jan. 2015.

[20] Z. Pi, J. Choi, and R. W. Heath, Jr., "Millimeter-wave gigabit broadband evolution toward 5G: Fixed access and backhaul," *IEEE Commun. Mag.*, vol. 54, no. 4, pp. 138–144, Apr. 2016.

[21] A. Douik, H. Dahrouj, T. Y. Al-Naffouri, and M. S. Alouini, "Hybrid radio/free-space optical design for next generation backhaul systems," *IEEE Trans. Commun.*, vol. 64, no. 6, pp. 2563–2577, Jun. 2016.

[22] H. Dahrouj, A. Douik, F. Rayal, T. Y. Al-Naffouri, and M.-S. Alouini, "Cost-effective hybrid RF/FSO backhaul solution for next generation wireless systems," *IEEE Wireless Commun.*, vol. 22, no. 5, pp. 98–104, Oct. 2015.

[23] A. Douik, H. Dahrouj, T. Y. Al-Naffouri, and M. S. Alouini, "Cost-effective backhaul design using hybrid radio/free-space optical technology," in *Proc. IEEE Int. Conf. Commun. Workshop (ICCW)*, Jun. 2015, pp. 7–12.

[24] Facebook. (Jul. 2017). *Connectivity Lab*. [Online]. Available: https://info.internet.org/en/story/connectivity-lab/

[25] T. Peyronel, K. J. Quirk, S. C. Wang, and T. G. Tiecke, "Luminescent detector for free-space optical communication," *Optica*, vol. 3, no. 7, pp. 787–792, Jul. 2016. [Online]. Available: http://www.osapublishing.org/optica/abstract.cfm?URI=optica-3-7-787

[26] A. G. Talmor, H. Harding, and C.-C. Chen, "Two-axis gimbal for air-to-air and air-to-ground laser communications," *Proc. SPIE*, vol. 9739, pp. 97390G-1–97390G-7, 2016. [Online]. Available: http://dx.doi.org/10.1117/12.2218097

[27] S. Guo, M. Guo, V. C. M. Leung, S. Yu, and Y. Xiang, "On the multicast lifetime of WANETs with multibeam antennas: Formulation, algorithms, and analysis," *IEEE Trans. Comput.*, vol. 63, no. 8, pp. 1988–2001, Aug. 2014.

[28] J. E. Wieselthier, G. D. Nguyen, and A. Ephremides, "The impact of directional antennas on energy-aware, session-based multicasting in ad hoc wireless networks," in *Proc. Commun. Netw.-Centric Oper., Creating Inf. Force. IEEE Military Commun. Conf. (MILCOM)*, vol. 2. Oct. 2001, pp. 947–951.

[29] J. E. Wieselthier, G. D. Nguyen, and A. Ephremides, "Energy-aware wireless networking with directional antennas: The case of session-based broadcasting and multicasting," *IEEE Trans. Mobile Comput.*, vol. 1, no. 3, pp. 176–191, Jul. 2002.

[30] J. E. Wieselthier, G. D. Nguyen, and A. Ephremides, "Energy-limited wireless networking with directional antennas: The case of session-based multicasting," in *Proc. 21st Annu. Joint Conf. IEEE Comput. Commun. Soc. (INFOCOM)*, vol. 1. Jun. 2002, pp. 190–199.

[31] S. Guo, M. Guo, and V. Leung, "Exploring the multicast lifetime capacity of wanets with directional multibeam antennas," in *Proc. IEEE INFOCOM*, Apr. 2009, pp. 2686–2690.

[32] R. Vaishampayan, J. J. Garcia-Luna-Aceves, and K. Obraczka, "Efficient multicasting in multi-hop ad hoc networks using directional antennas," in *Proc. IEEE Int. Conf. Mobile Adhoc Sensor Syst. Conf.*, Nov. 2005, pp. 9 pp.–664.

[33] C.-C. Shen, Z. Huang, and C. Jaikaeo, "Directional broadcast for mobile ad hoc networks with percolation theory," *IEEE Trans. Mobile Comput.*, vol. 5, no. 4, pp. 317–332, Apr. 2006.

[34] A. Nasipuri, J. Mandava, H. Manchala, and R. E. Hiromoto, "On-demand routing using directional antennas in mobile ad hoc networks," in *Proc. 9th Int. Conf. Comput. Commun. Netw.*, Oct. 2000, pp. 535–541.

[35] Y. T. Hou, Y. Shi, H. D. Sherali, and J. E. Wieselthier, "Online lifetime-centric multicast routing for ad hoc networks with directional antennas," in *Proc. 24th Annu. Joint Conf. IEEE Comput. Commun. Soc. (INFOCOM)*, vol. 1. Mar. 2005, pp. 761–772.

[36] Y. T. Hou, Y. Shi, H. D. Sherali, and J. E. Wieselthier, "Multicast communications in ad hoc networks using directional antennas: A lifetime-centric approach," *IEEE Trans. Veh. Technol.*, vol. 56, no. 3, pp. 1333–1344, May 2007.

[37] S. Guo, O. Yang, and V. Leung, "Approximation algorithms for longest-lived directional multicast communications in WANETs," in *Proc. 8th ACM Int. Symp. Mobile Ad Hoc Netw. Comput. (MobiHoc)*, 2007, pp. 190–198. [Online]. Available: http://doi.acm.org/10.1145/1288107.1288133

[38] S. Guo, V. Leung, and X. Jiang, "Distributed approximation algorithms for longest-lived multicast in wanets with directional antennas," *IEEE Trans. Wireless Commun.*, vol. 9, no. 7, pp. 2227–2237, Jul. 2010.

[39] S. Guo, V. C. M. Leung, and O. W. W. Yang, "WSNp1-7: Distributed multicast algorithms for lifetime maximization in wireless ad hoc networks with omni-directional and directional antennas" in *Proc. IEEE GLOBECOM*, Nov. 2006, pp. 1–5.

[40] S. Guo, M. Dong, and M. Guo, "Performance analysis of heuristic algorithms for lifetime-aware directional multicasting in wireless ad hoc networks," in *Proc. 22nd Int. Conf. Adv. Inf. Netw. Appl.-Workshops (AINA Workshops)*, Mar. 2008, pp. 1311–1316.

[41] S. Guo and O. Yang, "Multicast lifetime maximization for energy-constrained wireless ad-hoc networks with directional antennas," in *Proc. IEEE Global Telecommun. Conf. (GLOBECOM)*, vol. 6. Nov. 2004, pp. 4120–4124.

[42] X. Liu, S. Guo, and A. E. Saddik, "Communication complexity evaluation for longest-lived directional multicasting in WANETs," in *Proc. IEEE Int. Conf. Commun.*, May 2008, pp. 3029–3033.

[43] S. Guo and O. Yang, "Formulation of optimal tree construction for maximum lifetime multicasting in wireless ad-hoc networks with adaptive antennas," in *Proc. IEEE Int. Conf. Commun. (ICC)*, vol. 5. May 2005, pp. 3370–3374.

[44] S. Guo and O. Yang, "Improving energy efficiency for multicasting in wireless ad-hoc networks with adaptive antennas," in *Proc. IEEE Int. Conf. Wireless Mobile Comput., Netw. Commun. (WiMob)*, vol. 3. Aug. 2005, pp. 344–351.

[45] H. Park, S. Park, T. Song, and S. Pack, "An incremental multicast grouping scheme for mmWave networks with directional antennas," *IEEE Commun. Lett.*, vol. 17, no. 3, pp. 616–619, Mar. 2013.

[46] M. Khan and M. Yuksel, "Maintaining a free-space-optical communication link between two autonomous mobiles," in *Proc. IEEE Wireless Commun. Netw. Conf. (WCNC)*, Apr. 2014, pp. 3154–3159.

[47] M. Khan, G. Winkelmaier, and M. Yuksel, "In-band autonomous maintenance of mobile free-space-optical links: A prototype," in *Proc. IEEE Int. Conf. Commun. Workshops (ICC)*, May 2016, pp. 157–162.

[48] M. Khan, M. Yuksel, and G. Winkelmaier, "GPS-free maintenance of a free-space-optical link between two autonomous mobiles," *IEEE Trans. Mobile Comput.*, vol. 16, no. 6, pp. 1644–1657, Jun. 2016.

[49] S. Bhunia, M. Khan, S. Sengupta, and M. Yuksel, "LOS discovery for highly directional full duplex RF/FSO transceivers," in *Proc. IEEE Military Commun. Conf. (MILCOM)*, Nov. 2016, pp. 337–342.

[50] M. Khan, S. Bhunia, M. Yuksel, and S. Sengupta, "LOS discovery in 3D for highly directional transceivers," in *Proc. IEEE Military Commun. Conf. (MILCOM)*, Nov. 2016, pp. 325–330.

[51] J. Derenick, C. Thorne, and J. Spletzer, "On the deployment of a hybrid free-space optic/radio frequency (FSO/RF) mobile ad-hoc network," in *Proc. IEEE/RSJ Int. Conf. Intell. Robots Syst. (IROS)*, Aug. 2005, pp. 3990–3996.

[52] J. Derenick, C. Thorne, and J. Spletzer, "Hybrid free-space optics/radio frequency (FSO/RF) networks for mobile robot teams," in *Multi-Robot Systems. From Swarms to Intelligent Automata*, vol. 3. Dordrecht, The Netherlands: Springer, 2005, pp. 263–268.

[53] P. LoPresti, H. Refai, J. Sluss, and I. Varela-Cuadrado, "Adaptive divergence and power for improving connectivity in free-space optical mobile networks," *Appl. Opt.*, vol. 45, no. 25, pp. 6591–6597, 2006. [Online]. Available: https://www.osapublishing.org/abstract.cfm?uri=ao-45-25-6591

[54] M. Bilgi and M. Yuksel, "Multi-transceiver simulation modules for free-space optical mobile ad hoc networks," *Proc. SPIE*, vol. 7705, p. 77050B, May 2010.

[55] M. Bilgi and M. Yuksel, "Capacity scaling in free-space-optical mobile ad hoc networks," *Ad Hoc Netw.*, vol. 12, pp. 150–164, Jan. 2014. [Online]. Available: http://dx.doi.org/10.1016/j.adhoc.2011.12.003

[56] A. Sevincer, M. Bilgi, M. Yuksel, and N. Pala, "Prototyping multi-transceiver free-space optical communication structures," in *Proc. IEEE Int. Conf. Commun. (ICC)*, May 2010, pp. 1–5.

[57] M. Bilgi and M. Yuksel, "Multi-element free-space-optical spherical structures with intermittent connectivity patterns," in *Proc. INFOCOM Workshops*, Apr. 2008, pp. 1–4.

[58] M. Yuksel, J. Akella, S. Kalyanaraman, and P. Dutta, "Free-space-optical mobile ad hoc networks: Auto-configurable building blocks," *Wireless Netw.*, vol. 15, no. 3, pp. 295–312, 2007. [Online]. Available: http://dx.doi.org/10.1007/s11276-007-0040-y

[59] M. Bilgi and M. Yuksel, "Packet-based simulation for optical wireless communication," in *Proc. 17th IEEE Workshop Local Metropolitan Area Netw. (LANMAN)*, May 2010, pp. 1–6.

[60] J. Akella, C. Liu, D. Partyka, M. Yuksel, S. Kalyanaraman, and P. Dutta, "Building blocks for mobile free-space-optical networks," in *Proc. 2nd IFIP Int. Conf. Wireless Opt. Commun. Netw. (WOCN)*, Mar. 2005, pp. 164–168.

[61] M. Bilgi and M. Yuksel, "Throughput characteristics of free-space-optical mobile ad hoc networks," in *Proc. 13th ACM Int. Conf. Modeling, Anal., Simulation Wireless Mobile Syst. (MSWIM)*, 2010, pp. 170–177. [Online]. Available: http://doi.acm.org/10.1145/1868521.1868549

[62] A. Sevincer and M. Yuksel, "Effective transceiver selection for mobile multi-directional free-space-optical modules," in *Proc. IEEE Wireless Commun. Netw. Conf. (WCNC)*, Apr. 2014, pp. 2988–2993.

[63] B. Nakhkoob, M. Bilgi, M. Yuksel, and M. Hella, "Multi-transceiver optical wireless spherical structures for MANETs," *IEEE J. Sel. Areas Commun.*, vol. 27, no. 9, pp. 1612–1622, Dec. 2009.

[64] Y. Jahir, M. Atiquzzaman, H. Refai, and P. G. LoPresti, "AODVH: Ad hoc on-demand distance vector routing for hybrid nodes," in *Proc. IEEE Int. Conf. Commun. (ICC)*, May 2010, pp. 1–5.

[65] Y. Jahir, M. Atiquzzaman, H. Refai, and P. G. LoPresti, "Performance evaluation of AODVH: An ad hoc networking scheme for hybrid nodes," in *Proc. 13th Int. Conf. Comput. Inf. Technol. (ICCIT)*, Dec. 2010, pp. 165–169.
[66] R. A. Nichols, A. R. Hammons, D. J. Tebben, and A. Dwivedi, "Delay tolerant networking for free-space optical communication systems," in *Proc. IEEE Sarnoff Symp.*, Apr. 2007, pp. 1–5.
[67] R. A. Nichols and A. R. Hammons, "DTN-based free-space optical and directional RF networks," in *Proc. IEEE Military Commun. Conf. (MILCOM)*, Nov. 2008, pp. 1–6.
[68] R. A. Nichols and A. R. Hammons, "Performance of DTN-based free-space optical networks with mobility," in *Proc. IEEE Military Commun. Conf. (MILCOM)*, Oct. 2007, pp. 1–6.
[69] R. A. Nichols, "QoI in DTN-based directional networks," in *Proc. IEEE Sarnoff Symp.*, Mar. 2009, pp. 1–5.
[70] V. Navda, A. P. Subramanian, K. Dhanasekaran, A. Timm-Giel, and S. Das, "MobiSteer: Using steerable beam directional antenna for vehicular network access," in *Proc. 5th Int. Conf. Mobile Syst., Appl. Services (MobiSys)*, 2007, pp. 192–205. [Online]. Available: http://doi.acm.org/10.1145/1247660.1247684
[71] A. Spyropoulos and C. S. Raghavendra, "Energy efficient communications in ad hoc networks using directional antennas," in *Proc. 21st Annu. Joint Conf. IEEE Comput. Commun. Soc.*, vol. 1. Jun. 2002, pp. 220–228.
[72] O. Awwad, A. Al-Fuqaha, B. Khan, and G. B. Brahim, "Topology control schema for better QoS in hybrid RF/FSO mesh networks," *IEEE Trans. Commun.*, vol. 60, no. 5, pp. 1398–1406, May 2012.
[73] R. R. Choudhury, X. Yang, R. Ramanathan, and N. F. Vaidya, "On designing MAC protocols for wireless networks using directional antennas," *IEEE Trans. Mobile Comput.*, vol. 5, no. 5, pp. 477–491, May 2006.
[74] R. R. Choudhury and N. H. Vaidya, *Impact of Directional Antennas on Ad Hoc Routing*. Berlin, Germany: Springer, 2003, pp. 590–600. [Online]. Available: http://dx.doi.org/10.1007/978-3-540-39867-7_57
[75] G. Zhang *et al.*, "Multicast capacity for vanets with directional antenna and delay constraint," *IEEE J. Sel. Areas Commun.*, vol. 30, no. 4, pp. 818–833, Apr. 2012.
[76] R. R. Choudhury, X. Yang, R. Ramanathan, and N. H. Vaidya, "Using directional antennas for medium access control in ad hoc networks," in *Proc. 8th Annu. Int. Conf. Mobile Comput. Netw. (MobiCom)*, 2002, pp. 59–70. [Online]. Available: http://doi.acm.org/10.1145/570645.570653
[77] T. ElBatt, T. Anderson, and B. Ryu, "Performance evaluation of multiple access protocols for ad hoc networks using directional antennas," in *Proc. IEEE Wireless Commun. Netw. (WCNC)*, vol. 2. Mar. 2003, pp. 982–987.
[78] Z. Huang, C.-C. Shen, C. Srisathapornphat, and C. Jaikaeo, "A busy-tone based directional MAC protocol for ad hoc networks," in *Proc. MILCOM*, vol. 2. Oct. 2002, pp. 1233–1238.
[79] Y.-B. Ko, V. Shankarkumar, and N. H. Vaidya, "Medium access control protocols using directional antennas in ad hoc networks," in *Proc. 19th Annu. Joint Conf. IEEE Comput. Commun. Soc. (INFOCOM)*, vol. 1. Mar. 2000, pp. 13–21.
[80] R. Ramanathan, "On the performance of ad hoc networks with beamforming antennas," in *Proc. 2nd ACM Int. Symp. Mobile Ad Hoc Netw. Comput. (MobiHoc)*, 2001, pp. 95–105. [Online]. Available: http://doi.acm.org/10.1145/501426.501430
[81] R. Ramanathan, J. Redi, C. Santivanez, D. Wiggins, and S. Polit, "Ad hoc networking with directional antennas: A complete system solution," *IEEE J. Sel. Areas Commun.*, vol. 23, no. 3, pp. 496–506, Mar. 2005.
[82] I. Rubin, Y.-Y. Lin, A. Baiocchi, F. Cuomo, and P. Salvo, "Vehicular backbone networking protocol for highway broadcasting using directional antennas," in *Proc. IEEE Global Commun. Conf. (GLOBECOM)*, Dec. 2013, pp. 4414–4419.
[83] S. Kuribayashi, Y. Sakumoto, H. Ohsaki, S. Hasegawa, and M. Imase, "Performance evaluation of epidemic broadcast with directional antennas in vehicular ad-hoc networks," in *Proc. IEEE/IPSJ Int. Symp. Appl. Internet*, Jul. 2011, pp. 260–265.
[84] C. Jaikaeo and C.-C. Shen, "Multicast communication in ad hoc networks with directional antennas," in *Proc. 12th Int. Conf. Comput. Commun. Netw.*, Oct. 2003, pp. 385–390.
[85] A. K. Das, R. J. Marks, M. El-Sharkawi, P. Arabshahi, and A. Gray, "Optimization methods for minimum power multicasting in wireless networks with sectored antennas," in *Proc. IEEE Wireless Commun. Netw. Conf.*, vol. 3. Mar. 2004, pp. 1299–1304.
[86] S. Guo, O. Yang, and V. Leung, "Joint optimization of energy consumption and antenna orientation for multicasting in static ad hoc wireless networks," *IEEE Trans. Wireless Commun.*, vol. 5, no. 9, pp. 2563–2568, Sep. 2006.
[87] M. E. Steenstrup, "Exploiting directional antennas to provide quality of service and multipoint delivery in mobile wireless networks," in *Proc. IEEE Military Commun. Conf. (MILCOM0*, vol. 2. Oct. 2003, pp. 987–992.
[88] K. Sundaresan, K. Ramachandran, and S. Rangarajan, "Optimal beam scheduling for multicasting in wireless networks," in *Proc. 15th Annu. Int. Conf. Mobile Comput. Netw. (MobiCom)*, 2009, pp. 205–216. [Online]. Available: http://doi.acm.org/10.1145/1614320.1614343
[89] A. K. Majumdar and J. C. Ricklin, *Free-Space Laser Communications, Principles and Advances*. New York, NY, USA: Springer, 2008.
[90] V. V. Vazirani, *Approximation Algorithms*. Berlin, Germany: Springer-Verlag, 2003.
[91] E. Balas, "The prize collecting traveling salesman problem: II. Polyhedral results," *Networks*, vol. 25, no. 4, pp. 199–216, 1995. [Online]. Available: http://dx.doi.org/10.1002/net.3230250406
[92] E. Balas, "The prize collecting traveling salesman problem," *Networks*, vol. 19, pp. 621–636, Oct. 1989. [Online]. Available: http://dx.doi.org/10.1002/net.3230190602
[93] E. Balas and C. H. Martin, "Combinatorial optimization in steel rolling," DIMACS, Rutgers Univ., Brunswick, NJ, USA, Tech. Rep. 91-18/RUTCOR Rep. 3-91, Apr. 1991, pp. 20–24.
[94] G. Hardy and E. Wright, *An Introduction to the Theory of Numbers*, 5th ed. London, U.K.: Oxford Univ. Press, 1979.
[95] L.-P. Bigras, M. Gamache, and G. Savard, "The time-dependent traveling salesman problem and single machine scheduling problems with sequence dependent setup times," *Discrete Optim.*, vol. 5, no. 4, pp. 685–699, 2008. [Online]. Available: http://www.sciencedirect.com/science/article/pii/S1572528608000339
[96] J.-C. Picard and M. Queyranne, "The time-dependent traveling salesman problem and its application to the tardiness problem in one-machine scheduling," *Oper. Res.*, vol. 26, no. 1, pp. 86–110, Feb. 1978. [Online]. Available: http://dx.doi.org/10.1287/opre.26.1.86

MICHAEL ATAKORA received the B.Sc. degree in telecommunications engineering from the Kwame Nkrumah University of Science and Technology, Ghana, in 2010, the M.Sc. degree in electrical engineering from Tuskegee University, USA, in 2013. He is currently pursuing the Ph.D. degree in electrical engineering and computer science, under the guidance of Dr. H. Chenji, with Ohio University, USA, with a focus on hybrid RF/FSO mobile ad hoc networks.

HARSHA CHENJI received the B.Tech. degree in electrical and electronics engineering from NITK Surathkal, India, in 2007, and the M.S. and Ph.D. degrees in computer engineering from Texas A&M University, in 2009 and 2014, respectively, advised by Prof. R. Stoleru. In 2014, he joined as a Post-Doctoral Researcher with the Wireless Networks Laboratory, headed by Prof. Z. J. Haas, Department of Computer Science, The University of Texas at Dallas. Since 2015, he has been an Assistant Professor with the School of Electrical Engineering and Computer Science, Ohio University, where he also leads the Wireless Systems Research Group. In 2016, he was selected for the 2016 Visiting Faculty Research Program by the Air Force Research Laboratory (Information Directorate), Rome, NY, USA. His general area of research is computer networking. His current research interests include free-space optical networks and wireless networks.